AD NUMBER

AD803195

NEW LIMITATION CHANGE

TO

Approved for public release, distribution unlimited

FROM

Distribution authorized to U.S. Gov't. agencies and their contractors; Critical Technology; NOV 1966. Other requests shall be referred to Air Force Weapons Lab., AFSC, Kirtland AFB, NM.

AUTHORITY

AFWL ltr, 30 Nov 1971

THEORETICAL CALCULATIONS OF THE PHENOMENOLOGY OF HE DETONATIONS

Volume I

William A. Whitaker, Captain, USAF
Edmund A. Nawrocki, Captain, USAF
Charles E. Needham
William W. Troutman

TECHNICAL REPORT NO. AFWL-TR-66-141, Vol. I
November 1966

AIR FORCE WEAPONS LABORATORY
Research and Technology Division
Air Force Systems Command
Kirtland Air Force Base
New Mexico

THEORETICAL CALCULATIONS OF THE PHENOMENOLOGY OF HE DETONATIONS

Volume I

William A. Whitaker, Captain, USAF
Edmund A. Nawrocki, Captain, USAF
Charles E. Needham
William W. Troutman

TECHNICAL REPORT NO. AFWL-TR-66-141, Vol. I

FOREWORD

This research was performed under Program Element 7.60.08.01.D, Project 5710, Subtask 1.027, and was funded by the Defense Atomic Support Agency (DASA).

Inclusive dates of research were 1 September 1965 to 1 June 1966. The report was submitted 27 October 1966 by the Project Officer, Captain William A. Whitaker, (WLRTH).

This report has been reviewed and is approved.

William A. Whitaker

WILLIAM A. WHITAKER
Captain, USAF
Project Officer

Ralph H. Pennington

RALPH H. PENNINGTON
Colonel, USAF
Chief, Theoretical Branch

Claude K. Stambaugh

CLAUDE K. STAMBAUGH
Colonel, USAF
Chief, Research Division

ABSTRACT

The phenomenology of two atmospheric high-explosive detonations were calculated theoretically. The first was a 20-short-ton spherical charge of TNT (loading density--1.56 gms/cc). The second was a methane-oxygen mixture (mole ratio 1 to 1.5) contained in a 55-ft-radius balloon. Both detonations took place at an altitude of 670 meters (ambient pressure 13.6 psi) with a reflecting surface 85 feet below burst point. The calculations, taken out to 300 milliseconds after detonations, were performed by using SAP, a one-dimensional Lagrangian hydrodynamic code and SHELL-OIL, a two-dimensional pure Eulerian hydrodynamic code. Volume II of this report contains the details of the results in graphical form. Included are pressure and density contours, velocity vector plots, and wave forms for 19 test stations.

This page intentionally left blank.

CONTENTS

ILLUSTRATIONS

TABLES

SECTION I

INTRODUCTION

The Air Force Weapons Laboratory is engaged in a series of theoretical calculations of the phenomenology of atmospheric nuclear weapon detonations. These calculations are based chiefly upon a series of large computer codes, to enable prediction from essentially first principles, of the phenomenology from microseconds to minutes after a detonation. The purpose of this undertaking is to provide a best theoretical picture of the phenomenology of atmospheric detonations for use in radar and re-entry vehicle vulnerability studies.

Three main codes are used in this program: SPUTTER, a one-dimensional radiation transport Lagrangian hydrodynamic code; SAP, a one-dimensional Lagrangian hydrodynamic code; and SHELL, a two-dimensional Eulerian hydrodynamic code. The first, SPUTTER, takes the radiative output directly from weapons design calculations, deposits the energy in air, and calculates the radiative and hydrodynamic growth of the fireball to a time of about one second. It uses a multi-frequency transport scheme involving typically 20 frequency groups. The output of this code is used as input to SAP, which calculates the hydrodynamic expansion of the shock wave at various angles to the horizontal. This calculation can proceed to great distances so that even the shock on the ground can be estimated, but it is chiefly important in the strong-shock region of interest in R/V vulnerability. The output of SPUTTER is also used as input to SHELL, which calculates fireball growth and rise to late times. The output of these codes is processed to give the desired observables such as pressure, temperature, and velocity.

The first shot so calculated was BLUEGILL, a high-altitude detonation of the DOMINIC-FISHBOWL nuclear test series. This particular shot was chosen because of the extremely fine field data available on it. The calculation, completed and reported (Ref 1 and 2), agreed with the field data to within experimental error and so has given considerable confidence in these codes to simulate atmospheric detonations.

In support of DISTANT PLAIN pre-shot planning, SAP and SHELL were modified to calculate the phenomenology of atmospheric HE detonations. A "burn" routine was included in SAP to provide the initial conditions for the calculation of

hydrodynamic shock growth. Besides providing the initial conditions and pressure-distance curves, output from SAP was also used as input to SHELL, which calculated the two-dimensional phenomena such as shock reflection, mach stem formation, and triple-point path.

There were two calculations each with a different energy source. The first was a 32-short-ton spherical charge of TNT detonated at a height of 26 meters which was 670 meters above sea level. The second was a 23.2-short-ton spherical charge of methane-oxygen mixed in a mole ratio of 1 to 1.5 detonated at the same height as the TNT.

Both calculations were run on SAP and SHELL, using SAP output as initial conditions for the SHELL calculation. The main features of the output are compared in as great detail as possible, and the hydrodynamic quantities are plotted for a large number of times in Volume II.

SECTION II

THE SAP CODE

SAP is a one-dimensional Lagrangian hydrodynamic code. It gets its name (Spherical Air PUFF) from another AFWL one-dimensional Lagrangian hydrodynamic code, PUFF (Ref 3 and 4) from which it evolved. PUFF in turn evolved from the LRL, Livermore, SHARP program. (Ref 5.)

SAP is not a general one-dimensional code but has been specialized to problems of atmospheric blast in order to increase its speed and accuracy. Written in the spherical coordinate system, it can calculate hydrodynamic shocks at any angle to the horizontal. It has a capability of over 1000 zones and is normally run without an automatic rezone. The mesh is rezoned periodically, combining zones "by hand" when necessary.

Other features of SAP are:

a. Radiation loss is possible, i.e., a certain amount of energy may be removed from every zone, each cycle, by a subroutine that determines the emission rate as a function of internal energy and density. (For the calculations reported here, this option was not used.)

b. A "continuous burn" routine based on Chapman-Jouguet theory was developed for SAP. This routine provides the conditions existing in the gaseous explosive products at the instant the detonation wave reaches the surface of the explosive charge. Such conditions provide more realistic starting conditions for the blast calculation than an isothermal sphere, which is more appropriate as a starting condition for a simulated nuclear burst calculation.

c. Shocks are calculated in the Von Neumann-Richtmeyer manner. SAP contains provisions for the use of a linear and or quadratic artificial viscosity.

d. SAP uses a real atmosphere that is stable under an R^{-2} gravity field, and an equation of state for air that is an empirical fit to Hilsenrath's data (Ref 6 and 7).

The equations solved in SAP are the partial differential equations for nonviscous, nonconducting compressible fluid flow written in Lagrangian form. These equations, including the equation of state are:

Mass

$$\left(\frac{\partial \rho}{\partial t}\right)_{x_0} + \rho \left(\frac{\partial u}{\partial x}\right)_t = 0 \tag{1}$$

Momentum

$$\left(\frac{\partial u}{\partial t}\right)_{x_0} + \frac{1}{\rho}\left(\frac{\partial p}{\partial x}\right)_t = g \tag{2}$$

Energy

$$\left(\frac{\partial I}{\partial t}\right)_{x_0} + p\left(\frac{\partial V}{\partial t}\right)_{x_0} = s \tag{3}$$

Equation of State

$$p = p(\rho, I) \tag{4}$$

where ρ = density in gms/cm^3

u = velocity in cm/sec

p = pressure in dynes/cm^2

I = specific internal energy in ergs/gm

V = specific volume in cm^3/gm

$= 1/\rho$

s = energy source in ergs/gm/sec

x = Eulerian coordinate in cm (position of a point of fluid relative to some external reference frame)

x_0 = Lagrangian coordinate (permanent lable attached to each moving point of fluid)

g = acceleration due to some external body force in cm/sec^2 (e.g. gravity)

t = time in seconds

and where the subscripts above denote what is being held constant in each derivative.

The finite difference approximations to the above equations, as used in SAP, are obtained in the usual manner. The fluid is divided into a mesh of fluid elements. Pressures, densities, and specific internal energies are defined at zone centers. Velocities and positions are defined at zone boundaries. See figure 1.

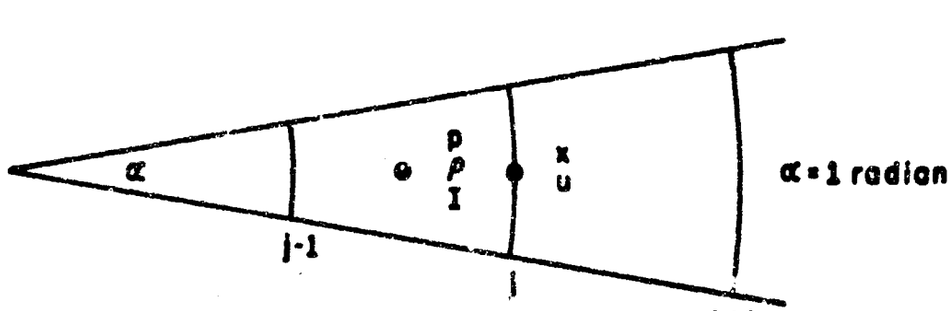

Figure 1. The SAP Mesh.

The finite difference equations are explicit time and space centered equations. The time centering is achieved in an explicit scheme by defining the velocity and coordinates of the mesh points a half cycle apart in time. The finite difference equations are written:

Momentum

$$u_j^{(n+1/2)} = u_j^{(n-1/2)} + \left[\frac{\left(p_{j-1/2}^{(n)} - p_{j+1/2}^{(n)}\right) + \left(q_{j-1/2}^{(n-1/2)} - q_{j+1/2}^{(n-1/2)}\right)}{1/2\left[\rho_{j-1/2}^{(n)}\left(x_j^{(n)} - x_{j-1}^{(n)}\right) + \rho_{j+1/2}^{(n)}\left(x_{j+1}^{(n)} - x_j^{(n)}\right)\right]} + g \right] \cdot \frac{\Delta t^{(n+1/2)} + \Delta t^{(n-1/2)}}{2} \tag{5}$$

Transformation

$$x_j^{(n+1)} = x_j^{(n)} + u_j^{(n+1/2)}\ \Delta t^{(n+1/2)} \tag{6}$$

Continuity

$$\rho_{j-1/2}^{(n+1)} = \frac{\rho_{j-1/2}^{(o)}\left[\left(x_j^{(o)}\right)^3 - \left(x_{j-1}^{(o)}\right)^3\right]}{\left(x_j^{(n+1)}\right)^3 - \left(x_{j-1}^{(n+1)}\right)^3} \tag{7}$$

Energy

$$I_{j-1/2}^{(n+1)} = I_{j-1/2}^{(n)} - \frac{p_2 + p_{j-1/2}^{(n)} + 2q_{j-1/2}^{(n+1/2)}}{2 - \frac{p_1 - p_2}{p_{j-1/2}^{(n)}}}\left(v_j^{(n+1)} - v_j^{(n)}\right) + s_{j-1/2}^{(n+1/2)}\ \Delta t^{(n+1/2)} \tag{8}$$

Equation of State

$$p_{j-1/2}^{(n+1)} = p\left(\rho_{j-1/2}^{(n+1)} \quad I_{j-1/2}^{(n+1)}\right) \tag{9}$$

where the energy equation is the simultaneous solution of the first law of thermodynamics,

$$I^{(n+1)} = I^{(n)} - 1/2 \left(p^{(n+1)} + p^{(n)}\right) dV \tag{10}$$

and the equation of state,

$$p^{(n+1)} = p\left(\rho^{(n+1)}, I^{(n+1)}\right) \tag{11}$$

and where

$$p_2 = p\left(\rho^{(n+1)}, I^{(n)}\right) \tag{12}$$

$$p_1 = p\left(\rho^{(n+1)}, I^{(n)} - p^{(n)} dV\right) \tag{13}$$

See reference 4.

The artificial viscosity term is given by

$$q = \begin{cases} \rho \Delta u \left(-c_1 cs + (c_0)^2 \Delta u\right) & \text{if } \frac{\partial V}{\partial t} \leq 0 \text{ and } \frac{\partial u}{\partial x} < 0 \\ 0 & \text{if } \frac{\partial V}{\partial t} > 0 \text{ or } \frac{\partial u}{\partial x} \geq 0 \end{cases} \tag{14}$$

which in finite difference form becomes

$$q_{j-1/2}^{(n+1/2)} = \rho_{j-1/2}^{(n+1)} \left(u_j^{(n+1/2)} - u_{j-1}^{(n+1/2)}\right) \left[-c_1 \, cs_{j-1/2}^{(n)} + c_0^{\,2} \left(u_j^{(n+1/2)} - u_{j-1}^{(n+1/2)}\right)\right] \tag{15}$$

if $\left(V_{j-1/2}^{(n+1)} - V_{j-1/2}^{(n)}\right) \leq 0$ and $\left(u_j^{(n+1/2)} - u_{j-1}^{(n+1/2)}\right) < 0$

and $q_{j-1/2}^{(n+1/2)} = 0$

if $\left(V_{j-1/2}^{(n+1)} - V_{j-1/2}^{(n)}\right) > 0$ or $\left(u_j^{(n+1/2)} - u_{j-1}^{(n+1/2)}\right) \geq 0$ (16)

where cs is the local sound speed, c_1 is the coefficient of linear viscosity (= 0.5), c_0 is the coefficient of quadratic viscosity (=1.8). The subscripts (j's) above are the Lagrangian coordinates and the superscripts (n's) refer to time such that $t^{(n+1)} = t^{(n)} + \Delta t^{(n+1/2)}$.

The SAP calculation advances explicitly in steps or cycles. That is, the zone quantities are calculated for the next time in terms of those at the present time. The order of calculation proceeds in the same sequence as the finite difference equations are presented:

a. A time step is calculated such that $\Delta t^{(n+1/2)}$ is the minimum of all

$$\frac{x_j - x_{j-1}}{2c_1 cs + 2c_0{}^2 |\Delta u| + cs} \text{ and } \Delta t^{(n-1/2)} \text{ (Ref 3)}$$

b. The momentum equation is solved.

c. Transformation is accomplished.

d. $q^{(n+1/2)}$'s are calculated.

e. The energy equation is solved.

f. $p^{(n+1)}$'s are calculated.

g. Edits are performed if desired.

SAP being a Lagrangian code enjoys all the advantages and suffers all the disadvantages characteristic of Lagrangian codes. Fine resolution is possible, since those regions requiring fine resolution retain their fine zoning since the coordinate system moves with the fluid. For this reason fine resolution is found in shock regions. However this is at the expense of resolution in rarefaction regions. The motion of material interfaces is also closely followed, since coordinate lines can be placed along them and will forever follow them.

Burn

The phenomenon of detonation from the time of its discovery, has been theoretically treated on the basis of shock-wave theory. Earliest observations of this phenomenon found that the fundamental property of detonations is that the detonation wave, for a given initial state of explosive substance or mixture, is propagated through that substance or mixture with a constant velocity. This property has been explained by Chapman and Jouguet whose work has resulted in a hydrodynamic theory of detonation.

Starting with the experimental fact that detonation is a stable and stationary process (being sustained by the energy of chemical reaction), they have shown that the detonation velocity is the minimum of all possible velocities for stationary conditions of propagation of a chemical reaction by a shock wave. That state, corresponding to the minimum value of velocity, has several interesting properties: the entropy has a minimum value on the Hugoniot curve and a maximum on the straight line in the p-v plane, which joins the corresponding point to the initial point, p_0, v_0. The detonation velocity in this state is equal to the sum of the velocity of the burned gas and the velocity of sound in the burned gas.

Therefore, based on the above properties of a Chapman-Jouguet detonation, a "burn" routine was written for SAP. Two methods of "burn" were used, both of which gave excellent results. In the first, the theoretical detonation velocity and the energy released per gram of explosive substance are entered as input numbers. Then

$$R^{(n+1)} = R^{(n)} + D\Delta t^{(n+1/2)} \tag{17}$$

and

$$\Delta I = \left[\left(R^{(n+1)}\right)^3 - \left(R^{(n)}\right)^3\right]\rho_k^{(n+1)}\, Q \tag{18}$$

where R = radius of the detonation wave in cm

D = detonation velocity in cm/sec

Δt = time step in sec

ΔI = energy released during the time step in ergs

ρ = density of the cell which is currently being "burned" in gms/cm^3

k = index of cell currently being "burned"

Q = energy liberated during detonation in ergs/gm

In the second method only the energy released per gram of explosive substance detonated is entered as an input number. When the transformation calculation is performed the radius of the detonation wave is similarly updated:

$$\bar{R} = R^{(n)} + \left[u_{k-1}^{(n+1/2)} + \frac{u_k^{(n+1/2)} - u_{k-1}^{(n+1/2)}}{x_k^{(n+1)} - x_{k-1}^{(n)}}\left(R^{(n)} - x_{k-1}^{(n+1)}\right)\right]\Delta t^{(n+1/2)} \tag{19}$$

Then the new radius of the detonation wave and the energy released is calculated:

$$R^{(n+1)} = \overset{\gamma}{R} + cs\Delta t^{(n+1/2)} \tag{20}$$

$$\Delta I = \left[\left(R^{(n+1)}\right)^3 - \overset{\gamma}{R}^3\right] \rho_k^{(n+1)} \, Q \tag{21}$$

where cs is the sound speed in the burned gas.

Therefore, the sequence of calculations with "burn" becomes:

a. Calculate $t^{(n+1/2)}$

b. Solve the momentum equation for all $u_j^{(n+1/2)}$

c. Update the Eulerian coordinates: $x_j^{(n+1)} = x_j^{(n)} + u_j^{(n+1/2)} \, t^{(n+1/2)}$

d. Calculate R as shown above if method 2 "burn" is used.

e. Calculate the new radius of detonation wave.

f. Calculate energy released due to the detonation of material in this time cycle and add the energy to the cell.

g. Solve the energy equation.

h. Calculate the new pressures from the equation of state.

i. Go to a and begin next cycle.

This sequence is followed until all the explosive matter has been detonated. Then the calculation becomes a "pure" hydrodynamic calculation.

SECTION III

THE SHELL CODE

SHELL is a versatile two-dimensional hydrodynamic code. It can be used to solve problems in any medium whose motions can be analyzed on the basis of inviscid hydrodynamic behavior of a cylindrically symmetric, compressible fluid. Some typical problems are: hypervelocity impact, cratering, vehicle re-entry, and detonations, underground, underwater, and in the atmosphere. A model and an equation of state for the medium of the problem are required by the code.

The Air Force Weapons Laboratory has two versions of the SHELL code. Both were developed at General Atomic by B. E. Freeman and W. E. Johnson primarily for hypervelocity impact calculations. The codes were modified at AFWL to calculate fireball rise and expansion.

The first and older of the two, SHELL-PIC, uses the Particle-in-Cell Method, developed by F. H. Harlow (Ref 8) at Los Alamos in 1955, to solve the hydrodynamic equations. The second, SHELL-OIL, is a continuous version of SHELL-PIC. Since early 1963, development of SHELL-OIL has been continued by J. M. Walsh and W. E. Johnson.

SHELL-PIC and SHELL-OIL have been in use at AFWL since 1961 and 1964, respectively.

In the following pages only SHELL-OIL will be described, since it was used in the calculations reported here.

The equations solved in SHELL are the partial differential equations for nonviscous, nonconducting compressible fluid flow. These equations, including the equation of state are

Mass

$$\left(\frac{\partial}{\partial t} + \vec{u}\cdot\nabla\right)\rho + \rho\nabla\cdot u = 0 \qquad (22)$$

Momentum

$$\rho\left(\frac{\partial}{\partial t} + \vec{u}\cdot\nabla\right)\vec{u} + \nabla p + \rho\nabla\phi = 0 \qquad (23)$$

Energy

$$\rho\left(\frac{\partial}{\partial t} + \vec{u}\cdot\nabla\right)E + \nabla\cdot p\vec{u} + \rho\vec{u}\cdot\nabla\phi = 0 \qquad (24)$$

Equation of State

$$p = p(\rho, I) \qquad (25)$$

where $\rho \equiv$ density in gms/cm^3

$\vec{u} \equiv$ velocity in cm/sec

$p \equiv$ pressure in dynes/cm^2

$E \equiv$ specific total energy in ergs/gm

$= I + 1/2\ u^2$

$I \equiv$ specific internal energy in ergs/gm

$t \equiv$ time in sec

$\phi \equiv$ potential of external force field in ergs/gm

a. SHELL-OIL

SHELL-OIL is a one material, pure Eulerian code. It solves the hydrodynamic equations by dividing the region occupied by the fluid into a mesh of fixed cells. The fluid is then described at any instant of time by specifying the velocity, density, and internal energy for each cell. These values are considered to be known at the center of each cell and constant over it. This forced homogeneity of the cell introduces a false diffusion, one disadvantage of Eulerian codes.

Other disadvantages of SHELL-OIL are the general inability of Eulerian codes to resolve fine detail moving with the fluid, since the mesh is fixed in space and the inability to follow material interfaces. However, Eulerian codes enjoy the major advantage of being able to solve the hydrodynamic equations even in the presence of large fluid distortions.

To begin a SHELL-OIL calculation, the problem must first be generated by CLAM, the generator code for SHELL. CLAM sets up the mesh, giving each cell dimensions and the following quantities: a radial and an axial velocity component, a mass, and a specific internal energy.

The cell quantities are derived from data entered in groups of packages. These data include the type of material, dimensions, velocity components, density, and specific internal energy of the package. To describe as many geometries and energy, density and velocity distributions as possible, CLAM places N^2 particles into each cell, where $1 \leq N \leq 20$ and is also included in the package data. Each cell is divided into N^2 equal parts, and a particle is placed at the center of each area. Taking this package data, a fit assigns each particle two velocity components, a density and a specific internal energy. Then the mass of each particle is computed: the density times the volume of that part of the cell containing the particle. The mass of the cell is the sum of the masses of all the particles in the cell. Both momentum components are calculated as the sum of the individual momentum components of each particle in the cell. The internal energy of each

cell is the sum of the internal energies of all the particles in the cell. Finally, these cell quantities are converted to two velocity components and specific internal energy.

The geometries available in CLAM are: rectangle, triangle, ellipse, perturbed ellipse and circle. These geometries are in the r-z plane and take their 3-dimensional counterparts upon rotation about the z-axis.

After all packages have been processed, CLAM puts all cell dimensions and quantities on tape. (If CLAM were generating the problem for a SHELL-PIC calculation, the coordinates and masses of each particle would also be written on this tape.) This output provides the starting conditions for the SHELL calculation.

Since SHELL-OIL is a one material code, an option to insert massless trace particles into the problem has been included in CLAM at AFWL. The purpose of these trace particles is to follow the detailed motion of a labeled material, to simulate the motion of a Lagrangian interface, or both. Therefore, the CLAM output also includes the coordinates of these trace particles on tape in addition to the cell quantities and dimensions for a SHELL-OIL calculation. These trace particles do not affect the hydrodynamics in any manner.

The SHELL calculation advances explicitly in steps or cycles. That is, the cell quantities are calculated for time $t + \Delta t$ in terms of those at time t. The solution of the hydrodynamic equations is divided into two phases. In the first, the Eulerian field functions are updated considering pressure effects alone, while neglecting material transport due to fluid motion. In the second phase, continuous mass flow across cell boundaries, new cell densities, velocities, and specific internal energies are calculated. Mass, momentum, and total energy are conserved. If mass flows out of the mesh, an automatic rezone increases the size of the mesh.

There are three time control conditions that govern the time step, Δt. They are:

a. The courant condition

b. The maximum of $\left|\frac{u}{\Delta r}\right|$ and $\left|\frac{v}{\Delta z}\right| < \frac{1}{\Delta t}$

c. A negative time step option

The first two conditions prohibit the transmission of a signal or mass across more than one cell in one time interval. This requirement is imposed by considerations of stability of the finite difference equations (Ref 8). The third condition will be discussed below.

After a time step has been determined, SHELL performs the first phase of the hydrodynamic calculation where the Eulerian description of the fluid is advanced. This is done according to a finite difference approximation to the hydrodynamic equations, Eq 22, 23, and 24.

Conservation of mass (Eq 22) is automatically satisfied by the fluid model. Mass, which leaves one cell, enters another and the change in mass is accordingly subtracted from the donor cell and added to the receiver cell. Mass is neither created nor destroyed.

Conservation of momentum and energy, (Eq 23 and 24), is treated as follows: the first phase considers the fluid at rest and determines only the contribution of the pressure terms to the time derivative. Therefore, the transport term (second term on the left-hand side) of each equation is dropped. Since the hydrodynamic quantities are defined at the cell centers, the equations in finite difference form become:

Momentum

$$\tilde{u}_k = u_k^{(n)} + \frac{1}{\rho_k^{(n)}} \frac{PL^{(n)} - PR^{(n)}}{\Delta r} \Delta t \tag{26}$$

$$\tilde{v}_k = v_k^{(n)} + \frac{1}{\rho_k^{(n)}} \frac{PB^{(n)} - PA^{(n)}}{\Delta z} \Delta t \tag{27}$$

Energy

$$\tilde{I}_k = I_k^{(n)} + \frac{p_k^{(n)}}{\rho_k^{(n)}} \left[\frac{VB^{(n)} - VA^{(n)} + \tilde{V}B - \tilde{V}A}{\Delta z} + \frac{2}{r_i + r_{i-1}} \frac{UL^{(n)} - UR^{(n)} + \tilde{U}L - \tilde{U}R}{\Delta r} \right] \frac{\Delta t}{2} \tag{28}$$

where

$$PL = \frac{p_k + p_{kL}}{2} \qquad PR = \frac{p_k + p_{kR}}{2}$$

$$PB = \frac{p_k + p_{kB}}{2} \qquad PA = \frac{p_k + p_{kA}}{2}$$

$$VB = \frac{v_k + v_{kB}}{2} \qquad VA = \frac{v_k + v_{kA}}{2}$$

$$UL = \frac{u_k\left(r_i + r_{i-1}\right) + u_{kL}\left(r_{i-1} + r_{i-2}\right)}{4}$$

$$UR = \frac{u_k\left(r_i + r_{i-1}\right) + u_{kR}\left(r_{i+1} + r_i\right)}{4}$$

and k is the index of the cell center and i is the index of the right-hand boundary of cell k. See figure 2.

Two passes, in succession, are made through the first phase of calculation of each cycle. In the first pass, tentative new values of velocity are calculated

for a full time step. The internal energy is updated by half a time step, using the old velocities. In the second pass, the internal energy is updated another half-time step, using the tentative new velocities calculated in the first pass. The energy equation is treated in this fashion, as proposed by Harlow (Ref 8), from considerations of stability as well as greatest accuracy in the behavior of fluid entropy. The energy of the system is conserved identically, even in the finite difference approach.

In both passes, the internal energy is checked to see if the updated value has become negative. If it has, an option exists to integrate back to the original configuration of the fluid at the beginning of the cycle by using the negative Δt. Then the integration goes forward again with a smaller Δt which has been calculated and which will keep the internal energy positive.

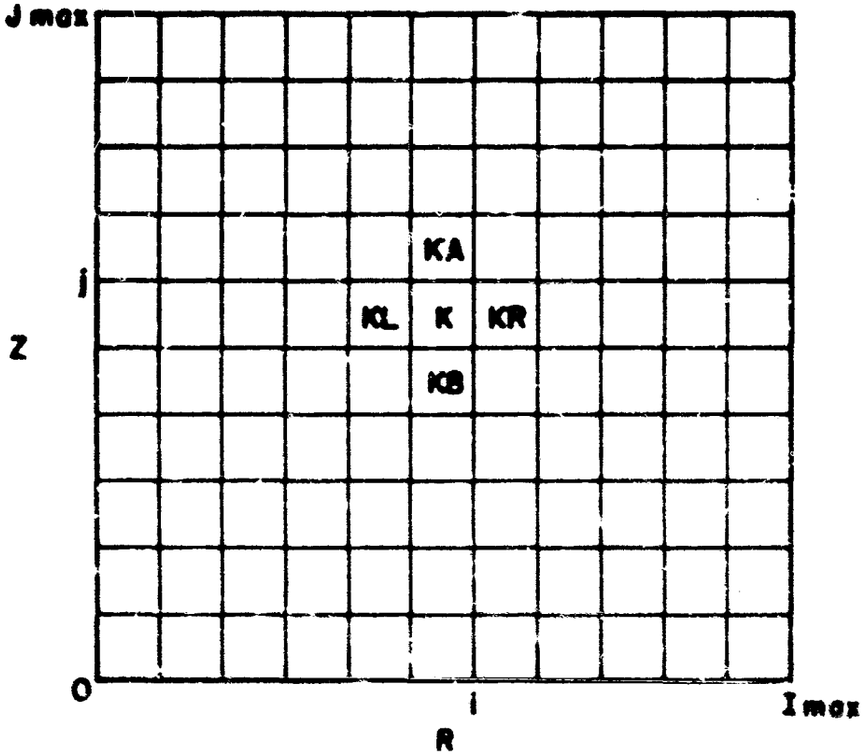

i is the right boundary of cell k

j is the top boundary of cell k

kA is the cell above cell k

etc.

Figure 2. The SHELL Mesh.

In the second phase of the hydrodynamic calculation, continuous mass transport is calculated according to the equation for the conservation of mass, which in finite difference form is:

$$\frac{\Delta\rho}{\Delta t} = -\left[\frac{r_{i-1}\rho_{i-1}u_{i-1}}{r_{i-1/2}\Delta r} - \frac{r_i\rho_i u_i}{r_{i-1/2}\Delta r} + \frac{\rho_{j-1}v_{j-1} - \rho_{j-1}}{\Delta z}\right] \qquad (29)$$

This can be rewritten to the following form, which is used by the code,

$$M_k^{(n+1)} = M_k^{(n)} + \pi\Delta t\left[\left(r_i^2 - r_{i-1}^2\right)\left(\bar{v}_B\rho_B - \bar{v}_T\rho_T\right) + 2\Delta z\left(r_{i-1}\bar{u}_L\rho_L - r_i\bar{u}_R\rho_R\right)\right] \quad (30)$$

Where $\bar{v}_B\rho_B \equiv$ mass flux across bottom face of cell K

$\bar{v}_T\rho_T \equiv$ mass flux across top face of cell K

$\bar{u}_L\rho_L \equiv$ mass flux across left face of cell K

$\bar{u}_R\rho_R \equiv$ mass flux across right face of cell K

and where the densities are those of the donor cells and the velocities are

$$\bar{v} = \frac{1/2\left(\tilde{v}_M + \tilde{v}_K\right)}{1 + \left(\tilde{v}_M - \tilde{v}_K\right)\frac{\Delta t}{\Delta z}}$$

$$\bar{u} = \frac{1/2\left(\tilde{u}_M + \tilde{u}_K\right)}{1 + \left(\tilde{u}_M - \tilde{u}_K\right)\frac{\Delta t}{\Delta r}}$$

where M signifies the index of the donor cell. The velocity weighing scheme used above is one that ensures stability in regions behind a shock front (Ref 9).

When mass transport is being calculated for a given cell, the transfer at the left and bottom faces is already available from the previous column sweep and cell below, respectively. Therefore, for a particular cell, the mass transport is calculated for the top and right faces only. After the masses transferred at all faces of a cell have been determined, the momenta and the total specific energy associated with these masses are computed. Then, by conserving both axial and radial momentum, the new velocities are calculated. The total energy carried by the transported masses is subtracted from the donor cell and added to the receiver cell. Then, by conserving total energy, the new internal energy of each cell is the difference between the new total energy and the new kinetic energy. The new specific internal energy is the new internal energy divided by the new mass.

$$M_k^{(n+1)} = M_k^{(n)} + \Delta M_B + \Delta M_L - \Delta M_T - \Delta M_R \quad (31)$$

$$v_k^{(n+1)} = \frac{M_k^{(n)} v_k + \Delta M_B v_M + \Delta M_L v_M - \Delta M_T v_M - \Delta M_R v_M}{M_k^{(n+1)}} \quad (32)$$

$$u_k^{(n+1)} = \frac{M_k^{(n)} u_k + \Delta M_B u_M - \Delta M_L u_M - \Delta M_T u_M - \Delta M_R u_M}{M_k^{(n+1)}} \quad (33)$$

$$I_k^{(n+1)} = \left\{ M_k^{(n)} \left[I_k + 1/2\left(u_k^2 + v_k^2 \right) \right] + \Delta M_B \left[I_M + 1/2\left(u_M^2 + v_M^2 \right) \right] \right.$$

$$+ \Delta M_T \left[I_M + 1/2\left(u_M^2 + v_M^2 \right) \right] - \Delta M_T \left[I_M + 1/2\left(u_M^2 + v_M^2 \right) \right]$$

$$\left. - \Delta M_R \left[I_M + 1/2\left(u_M^2 + v_M^2 \right) \right] \right\} / M_K^{(n+1)} \qquad (34)$$

Where ΔM_B, ΔM_L, ΔM_T, and ΔM_R are the masses, in gms transferred across the bottom, left, top, and right faces of cell K, respectively, and where the quantities enclosed in brackets and subscripted by M are the specific total energies of the donor cells. The above are the final values of velocity, mass, and specific internal energy for the cycle.

If any mass leaves the top, right, or bottom* boundaries, that mass and the associated energy are subtracted from the total mass and energy of the system respectively. If the mass leaving the mesh is a certain percentage of the mass of the cell from which it left, a flag is set to rezone the system. Additional flags are also set to indicate whether the top, bottom, and right boundaries, or any combination of these three, of the mesh have been crossed.

The automatic rezone for SHELL-OIL has been developed at AFWL. In rezone, a predetermined number of columns and or rows, depending whether the top, bottom, and or right boundaries have been crossed, are deleted. The remaining cells are expanded in size to fill the original geometry of the mesh. The mass of each expanded cell is the sum of the masses of those portions of the original cells which make up the new cell. By conserving momentum and total energy, new velocities and internal energies of the new cells are calculated. Then the same number of columns, rows, or both, that have previously been deleted are now added to the mesh thus regaining the original number of cells. Ambient conditions are given to these added cells The calculation is then resumed.

The calculation of mass transport in SHELL-OIL has another feature that removes preferential transfer caused by initial choice of indexing. If the mass

*There is also an option for a reflective bottom boundary as was used in the calculation reported here.

out the top and right would remove more than the mass in the cell, the code recalculates new mass transfer by a weighing procedure. The ΔM_R would be its fraction of the total mass out times the mass of the cell and ΔM_T would be its fraction of the total mass out times the mass of the cell. That is,

$$\Delta M_T = \frac{\Delta M_T}{\Delta M_T + \Delta M_R}\left(M_K^{(n)} + \Delta M_L + \Delta M_B\right) \tag{35}$$

$$\Delta M_R = \frac{\Delta M_R}{\Delta M_T + \Delta M_R}\left(M_K^{(n)} + \Delta M_L + \Delta M_B\right) \tag{36}$$

In this calculation ΔM_L and ΔM_B are considered zero if they are flowing into cell K so that the maximum mass that could flow out the top and right is $M_K^{(n)}$. However if ΔM_L and ΔM_B are flowing out of cell K, the cell is committed to deliver this mass and so the maximum mass that can flow out the top and right is $M_K^{(n)} + \Delta M_L + \Delta M_B$ (where ΔM_L and ΔM_B are negative signifying flow in negative direction).

After the final velocities for the cycle have been determined for all the cells in the mass transport phase of the calculation, trace particle movement is calculated. The trace particles play no part in the hydrodynamics of the system but are merely moved to new positions according to

$$x = x_0 + u'\Delta t \tag{37}$$

$$y = y_0 + v'\Delta t \tag{38}$$

The velocities used to move each particle are the local velocities at the location of the trace particle. They have values which are interpolated between the velocities of the cells whose centers surround the particle. The velocities are obtained by assuming a rectangle with the same dimensions as a cell to be located around the particle. This imaginary cell overlaps from one to four mesh cells, depending on the position of the particle in the mesh cell. Then the interpolated velocity is calculated as the weighted average of the cell velocities, the weighing being proportional to the overlap areas. Hence the motion of the trace particles follows the motion of material, or a Lagrangian interface, depending on how the particles were originally placed in the problem, and gives a picture of the flow pattern. After all trace particles have been moved, the calculations for the cycle have been completed, and the next cycle begins with the determination of a new time step.

b. Stability

The Eulerian equations used in the first phase of the calculation are unstable, since they do not contain the dissipative mechanism necessary for a finite difference technique to calculate shocks. Since shocks appear as mathematical surfaces on which such fluid properties as density, pressure, internal energy, and entropy have discontinuities, suitable boundary conditions (those provided by the Rankine-Hugoniot equations) are needed to connect the values of the above quantities on both sides of the shock. However, Von Neumann and Richtmeyer, (Ref 10), have shown that the hydrodynamic equations can be straightforwardly solved by numerical methods if an artificial dissipative term is introduced. This term smears the shock so that the surface of discontinuity is replaced by a thin layer in which the above quantities vary rapidly but continuously. Hence, the numerical calculation proceeds as if there were no shock at all and at the same time satisfying the Rankine-Hugoniot conditions.

The instability of the calculations in the first phase introduces the main source of entropy loss in the entire calculation. However, stable calculations can be made by SHELL, since errors introduced in the second phase have the effect of smoothing out the discontinuities.

Harlow (Ref 8) has shown that the treatment of mass movement in the second phase of the calculation produces dissipative effects that give stability to the calculation. He demonstrated this by expanding the difference equations in a Taylor series about some central space and time. The result was the original differential equations plus some additional terms that, in lowest order, have the appearance of true viscous and heat conduction terms. Hence they are called the effective viscosity and effective heat conduction.

Conservation of Mass

$$\frac{\partial \rho}{\partial t} + \frac{\partial (r\rho u)}{r\partial r} + \frac{\partial (\rho v)}{\partial z} = 0 \qquad (39)$$

Conservation of Momentum--r direction

$$\rho\left(\frac{\partial u}{\partial t} + u\frac{\partial u}{\partial r} + v\frac{\partial u}{\partial z}\right) + \frac{\partial p}{\partial r} = \frac{\partial}{r\partial r}\left(r\lambda_u \frac{\partial u}{\partial r}\right) + \frac{\partial}{\partial z}\left(\lambda_v \frac{\partial u}{\partial z}\right) \qquad (40)$$

Conservation of Momentum--z direction

$$\rho\left(\frac{\partial v}{\partial t} + u\frac{\partial v}{\partial r} + v\frac{\partial v}{\partial z}\right) + \frac{\partial p}{\partial z} = \frac{\partial}{r\partial r}\left(r\lambda_u \frac{\partial v}{\partial r}\right) + \frac{\partial}{\partial z}\left(\lambda_v \frac{\partial v}{\partial z}\right) \qquad (41)$$

Conservation of Energy

$$\rho\left(\frac{\partial I}{\partial t} + u\frac{\partial I}{\partial r} + v\frac{\partial I}{\partial z}\right) + p\left[\frac{\partial (ru)}{r\partial r} + \frac{\partial v}{\partial z}\right]$$

$$= \frac{\partial}{r\partial r}\left(r\lambda_u \frac{\partial I}{\partial r}\right) + \frac{\partial}{\partial z}\left(\lambda_v \frac{\partial I}{\partial z}\right) + \lambda_u\left[\left(\frac{\partial u}{\partial r}\right)^2 + \left(\frac{\partial v}{\partial r}\right)^2\right]$$

$$+ \lambda_v\left[\left(\frac{\partial u}{\partial z}\right)^2 + \left(\frac{\partial v}{\partial z}\right)^2\right] \qquad (42)$$

where

$$\lambda_u = 1/2\rho|u|\Delta r$$
$$\lambda_v = 1/2\rho|v|\Delta z$$

However, Bjork (Ref 11) has shown that any attempt to relate the terms appearing on the right-hand side of the equations above to distinct physical effects leads to many contradictions. Some are: the "effective viscosity" terms contain symmetric and antisymmetric elements; the origin of the symmetric elements is not viscous in nature; the presence of the antisymmetric elements just adds confusion to any attempted representation; the terms do not leave the flow equations in an invariant form; a heat conduction law is implied where heat flow is proportional to the gradient of specific internal energy rather than of temperature. Moreover, the values of these terms far exceed the magnitude of the analagous physical terms. Therefore, these terms cannot be thought of as anything except errors, but they do make SHELL a practical code.

The form of the effective viscosity suggests another limitation of the SHELL code. Since the viscous effects are proportional to the local mean fluid speed, in regions of low fluid speed the viscosity will become ineffective and the instabilities of the difference equation will cause an exponential growth of any perturbations to the solution. But as the velocities increase and become comparable to the local sound speed, the viscosity again takes effect to limit further growth of instability. Hence, the instability is bounded and calculations can be made. This effective viscosity is the main source of entropy production in the calculation.

SECTION IV

THE CALCULATION

The calculations reported here were performed on the CDC-6600 computer. Code development, calculation, and output analysis (plotting) required approximately 100 hours of computer time.

1. SAP-TNT

The SAP-TNT calculation was taken from 0 to 0.534 second. Initially, 800 zones were used. The first zone had a Δr of 0.12 cm, and the other 799 had Δr of 0.5 cm. The first 327 zones were TNT (32 short tons*). The initial conditions were: density--1.56 gm/cm^3, internal energy--0, velocity--0. Beyond these 327 zones, the remaining zones were the ambient atmosphere (670 meters altitude).

"Burn" method 1, as described previously, was used to detonate the TNT. The detonation velocity (corresponding to a loading density of 1.56 gms/cm^3) used was 6.81×10^5 cm/sec. The energy released per gram of TNT detonated was 4.264×10^{10} ergs/gm (Ref 12).

The LSZK equation of state for the detonation products of TNT (Ref 12) was used for the TNT zones that were "burned." For the unburned TNT, a compressional equation of state, which is an analytical fit to the Hugoniot for solid explosives, was used.

2. TNT-SHELL

SAP results at 6.62 milliseconds were scaled to 20 short tons of TNT and used as input for the SHELL calculation. As a result of scaling, the SHELL starting time became 5.66 milliseconds The SAP values for density, specific internal energy and velocity were fitted into the two-dimensional SHELL mesh containing a real (1962 standard) atmosphere.

A mesh 156 cells in the z-direction and 142 cells in the r-direction for a total of 22,152 cells was established. All cells except the bottom row of 142 cells comprised the active mesh. Each cell in the bottom row was 644 meters high and 30 cm wide. Each cell in the active mesh was a 30-cm square.

*This particular charge was chosen to save calculation time, since it was directly applicable to a proposed surface detonation of a hemispherical charge of 20 tons of TNT (assuming 20 percent energy loss to the ground) and scalable to Distant Plain event one.

Therefore, the overall mesh extended from sea-level to an altitude of 690.5 meters and out to a radius of 42.6 meters; and the active portion of the mesh from 644 meters (ground-level) to an altitude of 690.5 meters and out to a radius of 42.6 meters. The bottom boundary (ground-level at 644 meters) was reflective; whereas, the top and right boundaries were transmittive and thus subject to rezone in their respective directions. The left boundary (r = 0) was the axis of symmetry.

Data were entered into CLAM in two packages, each of which generated 25 particles per cell for the sole purpose of fitting the data into the SHELL mesh. The first package fitted the ambient atmosphere into the active mesh with the exception of those cells contained in a sphere whose center was on the z-axis at an altitude of 670 meters and whose radius was 16.55 meters. Into these cells the second package fitted the SAP results of velocity, density, and internal energy at 6.62 milliseconds (5.66 ms scaled).

Trace particles were introduced into the calculation in order to follow the TNT-air boundary. A Lagrangian interface of 921 particles was placed in a semi-circle to simulate the TNT-air boundary. The center of this circle was on the z-axis at an altitude of 670 meters, and the radius was 14.188 meters.

Also introduced into the calculation were 19 "test stations" where the over-pressures, dynamic pressures, impulses, and velocities were calculated for each cycle. The positions of these "test stations" were chosen to coincide with experimental stations. See table I and figure 3.

The equation of state used in the SHELL calculation was that of air, the same equation of state for air as used in SAP. This equation of state was used for all regions including those regions that contained TNT.

3. SAP-Methane

The SAP-methane calculation was taken from 0 to 1 second. Initially 800 zones were used in the calculation. The first zone had a Δr of 6.4 cm, and the other 799 had Δr of 5.0 cm. The first 335 zones contained the methane balloon (initial radius: 16.764 meters). The initial conditions were: density--1.07197×10^{-3} gms/cm^3, internal energy--2.1886×10^9 ergs/gm, velocity--0. Beyond these 335 zones, the remaining zones were the ambient atmosphere (670 meters altitude).

Table I

POSITION OF THE TEST STATIONS

Test Station	Range		Altitude	
	Meters	(Feet)	Meters	(Feet)
1	0		0	
2	7.62	(25)	0	
3	15.24	(50)	0	
4	24.38	(80)	0	
5	38.0	(125)	0	
6	50.0	(164)	0	
7	63.8	(209)	0	
8	78.0	(256)	0	
9	93.3	(306)	0	
10	26.0	(85)	2.8	
11	38.0	(125)	2.8	(9)
12	50.0	(164)	2.8	(9)
13	38.0	(125)	7.6	(25)
14	50.0	(164)	7.6	(25)
15	63.8	(209)	7.6	(25)
16	50.0	(164)	15.2	(50)
17	63.8	(209)	18.0	(59)
18	78.0	(256)	15.2	(50)
19	78.0	(256)	22.8	(75)

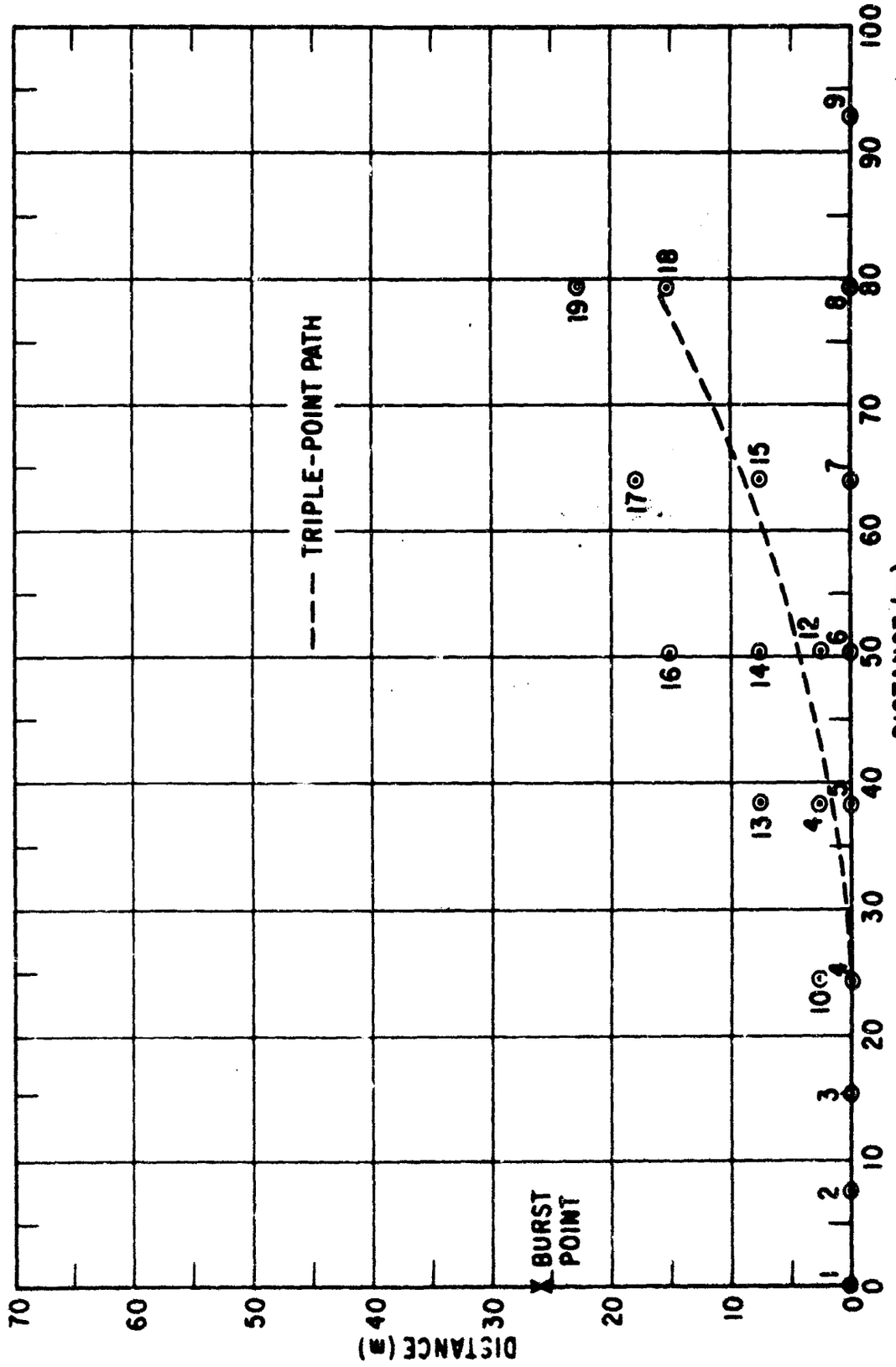

Figure 3. Position of the Test Stations.

"Burn" method 2, as described previously, was used to detonate the methane. The energy released per gram of methane-oxygen mixture detonated was 8.01×10^{10} ergs/gm (Ref 13). The detonation velocity calculated using "burn" method 2 was 2.743×10^5 cm/sec, as compared to a theoretical 2.752×10^5 cm/sec (Ref 13).

The ideal gas equation of state was used for the burned and unburned methane. For burned methane, the value of gamma used was 1.2136, while for unburned methane, the value of gamma used was 1.3986 (Ref 13).

4. Methane-SHELL

SAP-methane results at 8 milliseconds were used as input to SHELL. The SAP values for density, specific internal energy, and velocity as a function of position were fitted into the two-dimensional SHELL mesh. The geometry and boundary conditions were the same for the methane calculation as for the TNT calculation previously described.

Data were entered into CLAM in two packages, each of which generated 25 particles per cell for the sole purpose of fitting the data into the SHELL mesh. The first package fitted the ambient atmosphere into the active mesh with the exception of those cells contained in a sphere whose center was on the z-axis at an altitude of 670 meters and whose radius was 20.21 meters. Into these cells, the second package fitted the SAP results of velocity, density and internal energy as a function of position at 8 milliseconds.

Again trace particles were introduced into the calculation to represent the methane-air boundary. This Lagrangian interface consisted of 921 particles placed in a semicircle whose center was on the z-axis at an altitude of 670 meters and whose radius was 17.0 meters.

"Test stations" were introduced in the methane calculation. The location of these 19 stations were the same as for the TNT run. Again overpressures, dynamic pressures, impulses and velocities were calculated each cycle at these points. See table I.

5. LSZK Equation of State (Ref 12 and 14)

Landau, Stanyukovich, Zeldovich, and Kompaneets have developed an equation of state for the explosion products of a condensed explosive. They treated the highly compressed gas as a solid, likening the state of the detonation products immediately following completion of reaction, to the crystal lattice of the solid state. Further details concerning this equation of state are given in the above mentioned references.

The LSZK equation of state can be written

$$p = \frac{I\rho}{\alpha} + B\rho^{\nu}\left(1 - \frac{1}{\alpha(\nu - 1)}\right)$$

where p = pressure in dynes/cm^2

I = specific internal energy in ergs/gm

α, ν = dimensionless constants evaluated using experimental results

B = constant with dimensions (ML^{-3}) $1 - \nu$ also to be evaluated from experimental results.

Lutzky (Ref 12) gives the values of the above constants for TNT as

α = 2.9412

B/Q = 0.53562 $\left(\frac{gm}{cm^3}\right)^{1-\nu}$

ν = 2.78

where Q = 1018 calories/gm is the heat of detonation and the ideal gas value for the ratio of specific heats of the products at low densities was taken to be γ_i = 1.34.

This equation of state, as used in SAP for TNT, becomes

$$p = 0.34\ I\rho + 1.877 \times 10^{10}\rho^{2.78}$$

6. Equation of State for Air

The SAP and SHELL equation of state for air is a fit derived by AFWL (Ref 7) from the data of reference 6. Since the codes use energy and density as the independent variables and are pure hydrocodes, the only requirement on the equation of state is pressure as a function of energy and density. It is common to consider an effective gamma, which is $1 + P/\rho I$. The equation of state returns $(\gamma_{eff} - 1)$ from which is constructed the pressure. The region of interest of SAP and SHELL is chiefly molecular air and therefore the detailed equation of state is quite complicated. The present equation is a fairly complex formulation that gives all of the structure of this molecular region although not always with extremely high accuracy. The portion of the equation of state of interest in this problem is the 10^{-2} to 10^{0} density region below 2×10^{11} ergs/gm. In this region the fit is almost always within 5 percent with an average error of about 2 or 3 percent. It is however an interim equation and will be replaced soon by a more accurate formulation. The analytic expression of this equation of state is given below. I is specific energy in units of jerks/megagram or 10^{10} ergs/gm.

$$\gamma - 1 = \left\{0.161 + 0.255e^{-I/4.46}f_1 + 0.280e^{-I/6.63}\left(1 - f_1\right) + 0.137e^{-I/25.5}f_2 + 0.50f_3\right\}\left(\frac{\rho}{\rho_o}\right)^{a(I)}$$

$$a(I) = 0.48f_1\log_{10} I + 0.032\left(1 - f_1\right)\left(1 - f_2\right)\log_{10} I + 0.015f_2$$

$$f_1 = \left\{\exp\left[\frac{I - I_1}{\Delta I_1}\right] + 1\right\}^{-1} \qquad I_1 = 8.5 + 0.357 \log_{10}\left(\frac{\rho}{\rho_o}\right)$$

$$\Delta I_1 = 0.975\left(\frac{\rho}{\rho_o}\right)^{0.05}$$

$$f_2 = \left\{\exp\left[\frac{I_2 - I}{\Delta I_2}\right] + 1\right\}^{-1} \qquad I_2 = 45.0\left(\frac{\rho}{\rho_o}\right)^{0.015}$$

$$\Delta I_2 = 4.0\left(\frac{\rho}{\rho_o}\right)^{0.095}$$

$$f_3 = \left\{\left[\exp\frac{I_3 - I}{\Delta I_3}\right]\right\}^{-1} \qquad I_3 = 160$$

$$\Delta I_3 = 6$$

7. Atmospheric Model

The SHELL-OIL atmospheric model was also derived by AFWL from data contained in reference 15. To perform hydrodynamic calculations in the atmosphere, the atmosphere must be very stable, otherwise the first phase of the calculation will result in fictional vertical velocities. This condition is given by the hydrostatic equation

$$\frac{d[p(z)]}{dz} = -g(z)\,\rho(z)$$

The atmosphere is divided into 22 altitude groups from 0 to 700 km where the molecular temperature varies approximately linearly with altitude within each group. That is

$$T_m(z) = T_{m_o} + L\left(z - z_o\right)$$

where the subzero values refer to the base altitude of each group. Then by using the following relationships:

$$\rho(z) = \frac{M(z)p(z)}{RT(z)}$$

$$T_m(z) = \frac{M_o}{M(z)} T(z)$$

and

$$g(z) = \frac{g_o a^2}{(a + z)^2}$$

the hydrostatic equation becomes

$$-\frac{d[p(z)]}{p(z)} = \frac{g_o M_o a^2}{R} \frac{dz}{(a + z)^2 \left(T_{m_o} - Lz_o + Lz\right)}$$

where a ≡ the radius of the earth

g_o ≡ the acceleration due to gravity at sea level

M_o ≡ the molecular weight of air at sea level

and R ≡ the gas constant

Integration of the above between z and z_o results in the final form, which is used to interpolate pressures in an altitude group

$$\ln \frac{p}{p_o} = -\frac{g_o M_o a^2}{RL} \left\{ \left(a - \frac{T_{m_o} - Lz_o}{L}\right)^{-1} \frac{z_o - z}{(a + z)(a + z_o)} + \left(a - \frac{T_{m_o} - Lz_o}{L}\right)^{-2} \ln\left(\frac{a + z_o}{a + z} \frac{T_{m_o} - Lz_o + Lz}{T_{m_o}}\right) \right\}$$

To calculate the defining properties of the model atmosphere, the pressures at the base point of each altitude group and the molecular temperature at sea level were taken as constants. Then, starting at sea level, an iterative procedure was used to find the molecular temperature gradient, L (°K/km) in the first altitude group. Using L, thus determined, the molecular temperature of the base point of the next altitude group was calculated. Then the iterative procedure was again used to determine L for the second altitude group. With this technique the defining properties for the atmospheric model stable under the $1/R^2$ gravity field were determined. The final results are given in table II.

Table II

DEFINING PROPERTIES OF THE AFWL STANDARD ATMOSPHERE

Altitude z(Km)	Molecular scale temperature T_m (°K)	Gradient L (°K/cm)	Pressure p (dynes/cm^2)
0.0	288.1500	-6.492636×10^{-5}	1.01325×10^{6}
11.0	216.7310	-1.842590×10^{-7}	2.26999×10^{5}
20.0	216.5652	9.959301×10^{-6}	5.52930×10^{4}
32.0	228.5163	2.723233×10^{-5}	8.89063×10^{3}
47.0	269.3648	5.002971×10^{-6}	1.15851×10^{3}
52.0	271.8663	-2.051281×10^{-5}	6.22283×10^{2}
61.0	253.4048	-3.760658×10^{-5}	1.96917×10^{2}
79.0	185.7129	-8.818089×10^{-6}	1.24420×10^{1}
90.0	176.0130	3.986481×10^{-5}	1.64380
100.0	215.8779	3.882785×10^{-5}	3.00750×10^{-1}
110.0	254.7057	1.134533×10^{-4}	7.35440×10^{-2}
120.0	368.1590	1.927120×10^{-4}	2.52170×10^{-2}
150.0	946.2950	1.803651×10^{-4}	5.06170×10^{-3}
160.0	1126.6600	6.716274×10^{-5}	3.69430×10^{-3}
170.0	1193.8230	8.753717×10^{-5}	2.79260×10^{-3}
190.0	1368.8970	4.047483×10^{-5}	1.68520×10^{-3}
230.0	1530.7970	4.605377×10^{-5}	6.96040×10^{-4}
300.0	1853.1730	$2.825029 \quad 10^{-5}$	1.88380×10^{-4}
400.0	2135.6760	3.127025×10^{-5}	4.03040×10^{-5}
500.0	2448.3780	1.139442×10^{-5}	1.09570×10^{-5}
600.0	2561.9230	1.695913×10^{-5}	3.45020×10^{-6}
700.0	2731.5140	...	1.19180×10^{-6}

SECTION V

RESULTS

The output of both SHELL and SAP consists of values for pressure, velocity, density, and specific internal energy for each zone, every cycle. However, these quantities are recorded on output tape at selected times only.

To present this output in the most compact form, the quantities on the output tape are processed by a separate code that generates plots of the above variables. SAP plots consist of profiles only. SHELL plots consist of histograms, contours, and velocity vectors.

The overpressures, dynamic pressures, impulses, and velocities recorded at the "test stations" were also plotted as a function of time for each station.

Following normal procedure, SHELL and SAP peak shock pressures were extrapolated to find a "best" value for these quantities. This is usually necessary since numerical methods smear the shock over several zones. The extrapolation procedures for SAP and SHELL were developed based on a comparison of results of SAP and SHELL calculations, of a 1-KT detonation at sea level with the classical Taylor solution of a strong blast wave resulting from an intense explosion. Further comparisons in both strong and weak shock regions were made with the 1959 blast curve (Ref 17), which has been accepted to represent the experimental data from a 1-KT nuclear free-air burst at sea level. It was found that SAP peak pressures should be extrapolated to that radius where the maximum artificial viscosity occurs. This procedure holds for both strong and weak shock though for strong shocks the extrapolated pressures are not significantly different from the unextrapolated ones. It was also found that SHELL peak pressures should be extrapolated to that radius corresponding to 1/2 the peak overpressure for strong shocks (above 3 atm overpressure), but for weak shocks, the actual calculated peak pressure should be taken at that radius corresponding to 1/2 the peak overpressure. See figure 4.

The above procedures were used to extrapolate SAP and SHELL peak overpressures for the methane and TNT detonations. The extrapolated overpressures are plotted vs. radius and appear in figures 5 and 6.

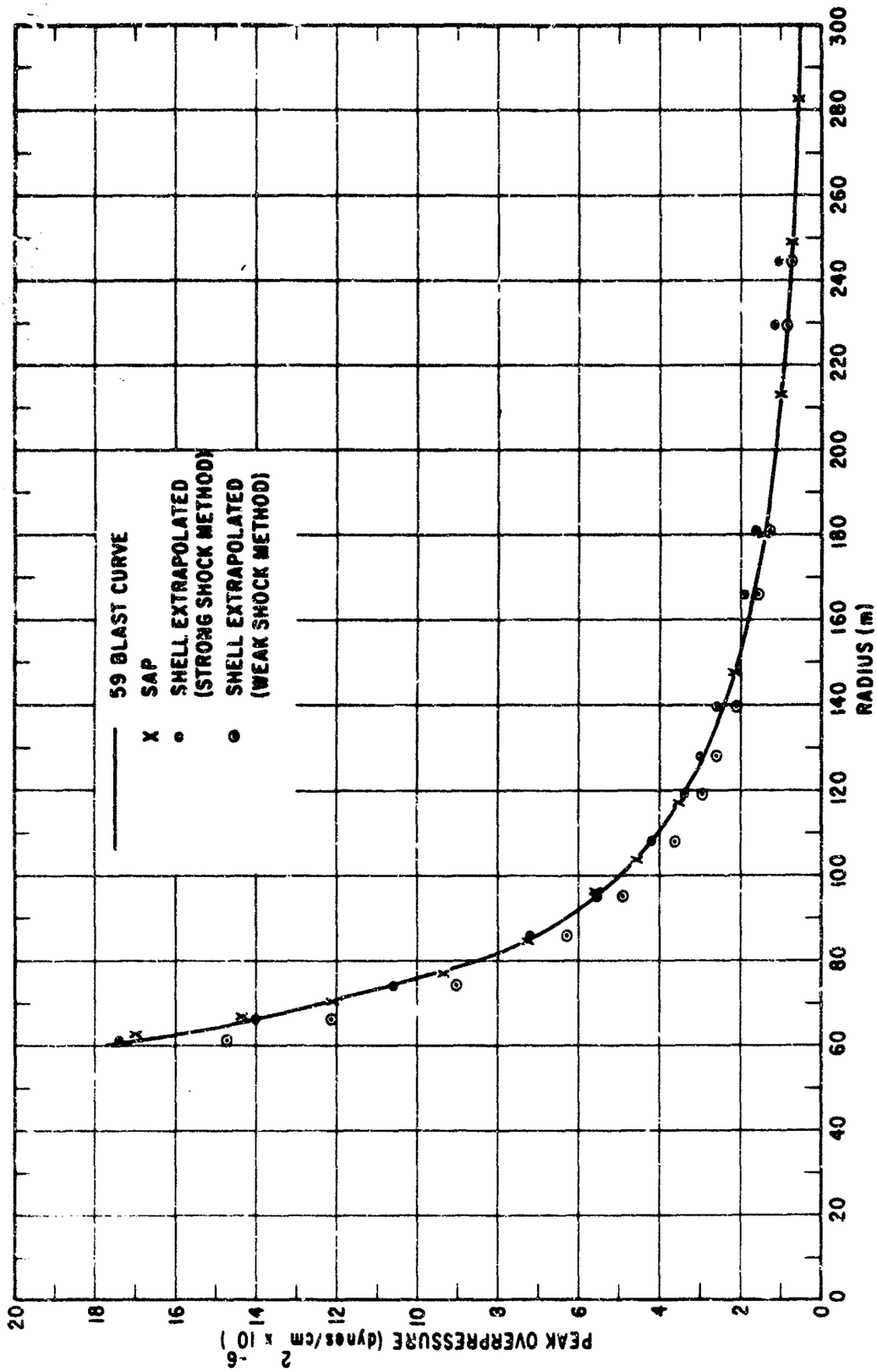

Figure 4. Results of Pressure Extrapolation.

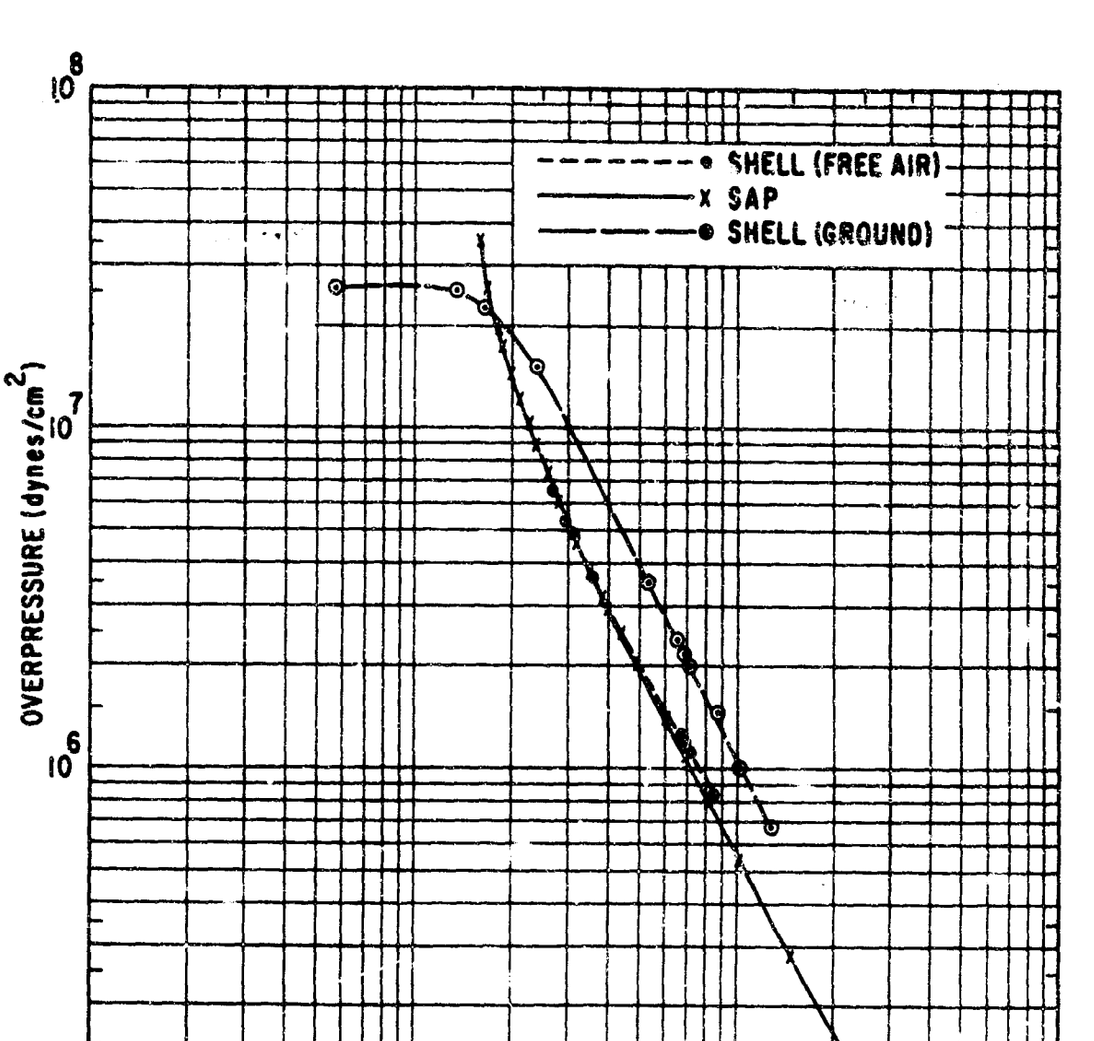

Figure 5. Methane Overpressure vs. Radius.

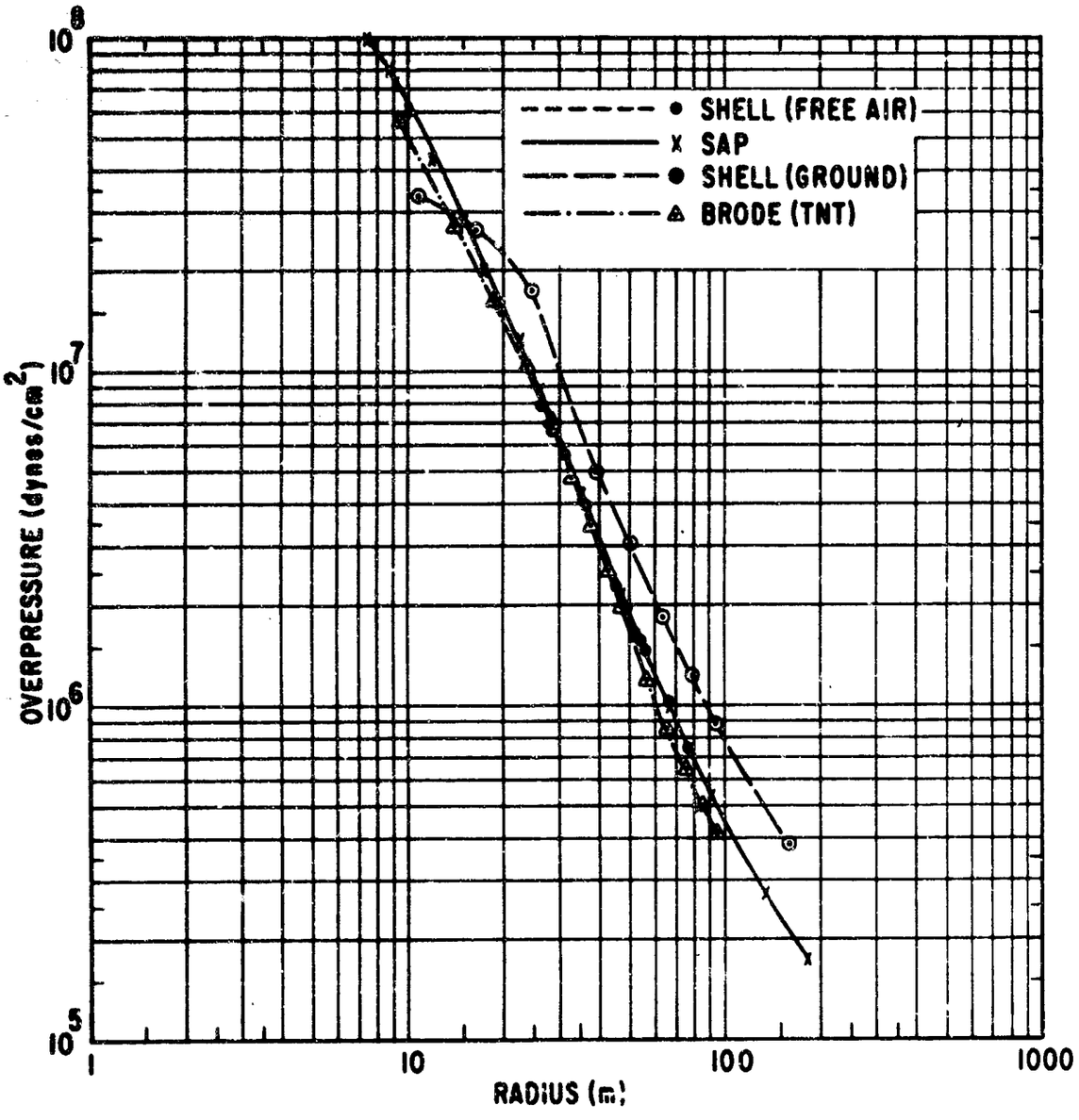

Figure 6. TNT Overpressure vs. Radius.

1. TNT

The following discussion of results of the TNT calculation applies to a scaled 20-short ton detonation.

The detonation wave in the SAP-TNT calculation reached a self-similar state very quickly with a peak pressure of 1.83×10^{11} dynes/cm^2. It reached the surface of the TNT at 0.2048 milliseconds. As the shock encountered the air, free expansion commenced. The peak pressure began to drop and a rarefaction wave started into the detonation products, toward the center. Meanwhile, the free-air shock was building up. The rarefaction wave reached the center at 0.6 milliseconds. At this point, the detonation products were "cold" and much more dense than the atmosphere surrounding them. However, the detonation products had high velocities and so acted like a piston pushing the atmosphere. A second shock formed in the detonation products just inside the TNT-air interface. It had a velocity smaller than the velocity of the interface so the second shock worked its way into the detonation products. However the net motion was still outward. At 16.3 milliseconds, the kinetic energy of the detonation products had dissipated to such an extent that the second shock began to move inward towards the center.

Meanwhile the main outward moving shock as calculated by SAP, had reflected off the surface of the earth at 13.36 milliseconds, with an incident overpressure of 140 psi, and a reflected overpressure of 730 psi. SHELL shows that after the main shock has proceeded along the ground for approximately one burst height (85 feet), the mach stem begins to form.

At 34 milliseconds the second shock reflects off the center and proceeds outward. It reflects off the ground at approximately 84 milliseconds with a reflected overpressure of 19 psi. This shock is very weak and is quickly dissipated. There are also other very weak shocks which are barely discernable.

The SHELL-TNT calculation indicates reflection of the main shock at the ground at 13.6 milliseconds with a reflected peak overpressure of 720 psi (extrapolated).

An auxiliary SAP calculation was performed, using the same SAP conditions which served as input to the SHELL calculation. (These conditions were deliberately chosen at a sufficiently advanced time when the density and internal energy of the detonation products were comparable to that of air.) For this run, the equation of state for air was used in all regions: both TNT and air. The purpose of this auxiliary calculation was to see whether there would be

significant differences, at these later times, between the results of a calculation using the LSZK equation of state for the TNT zones and those from one using the equation of state for air for the TNT zones. The results of this calculation showed no discernable difference in peak pressures or arrival times. Therefore, going from a two equation of state SAP calculation to a one equation of state SHELL calculation was justified. See figure 7.

2. Methane

The detonation wave in the SAP-methane calculation reached a self similar state very quickly with a peak pressure of 3.5×10^7 dynes/cm^2. It reached the surface of the balloon at 6.3 milliseconds.

As the shock wave hit the surface of the balloon, a second shock was reflected toward the center from the relatively higher density ambient air. This shock soon dissipated and the rarefaction wave started toward the center. The rarefaction wave reached the center at 18.2 milliseconds. The rarefaction was followed by a reflected shock which reached the center at 30 ms.

Meanwhile the main outward moving shock has reflected off the ground at 14.2 milliseconds with an incident overpressure of 7.43×10^6 dynes/cm^2 (108 psi). For this value of incident overpressure theoretical relationships give a reflected overpressure of 3.77×10^7 dynes/cm^2 (550 psi).

The second shock reached the ground at 62 milliseconds with a reflected overpressure of 25 psi. This shock is very weak and quickly dissipated.

The SHELL methane calculation indicated reflection of the main shock at the ground at 14.4 milliseconds with a reflected peak overpressure of 580 psi (extrapolated). From this time on, the two-dimensional phenomenology is similar to that for the TNT.

During the methane calculations the peak overpressures for stations 5 and 6 were lost. The loss of these peaks affect only the overpressure waveform and overpressure impulse for these stations. All other parameters are unaffected. The overpressure plots which appear for these stations (5 and 6) have only those points which were dumped on output tape to replace the missing points. The appendix to this report contains summary plots of information contained in the detailed plots of Volume II.

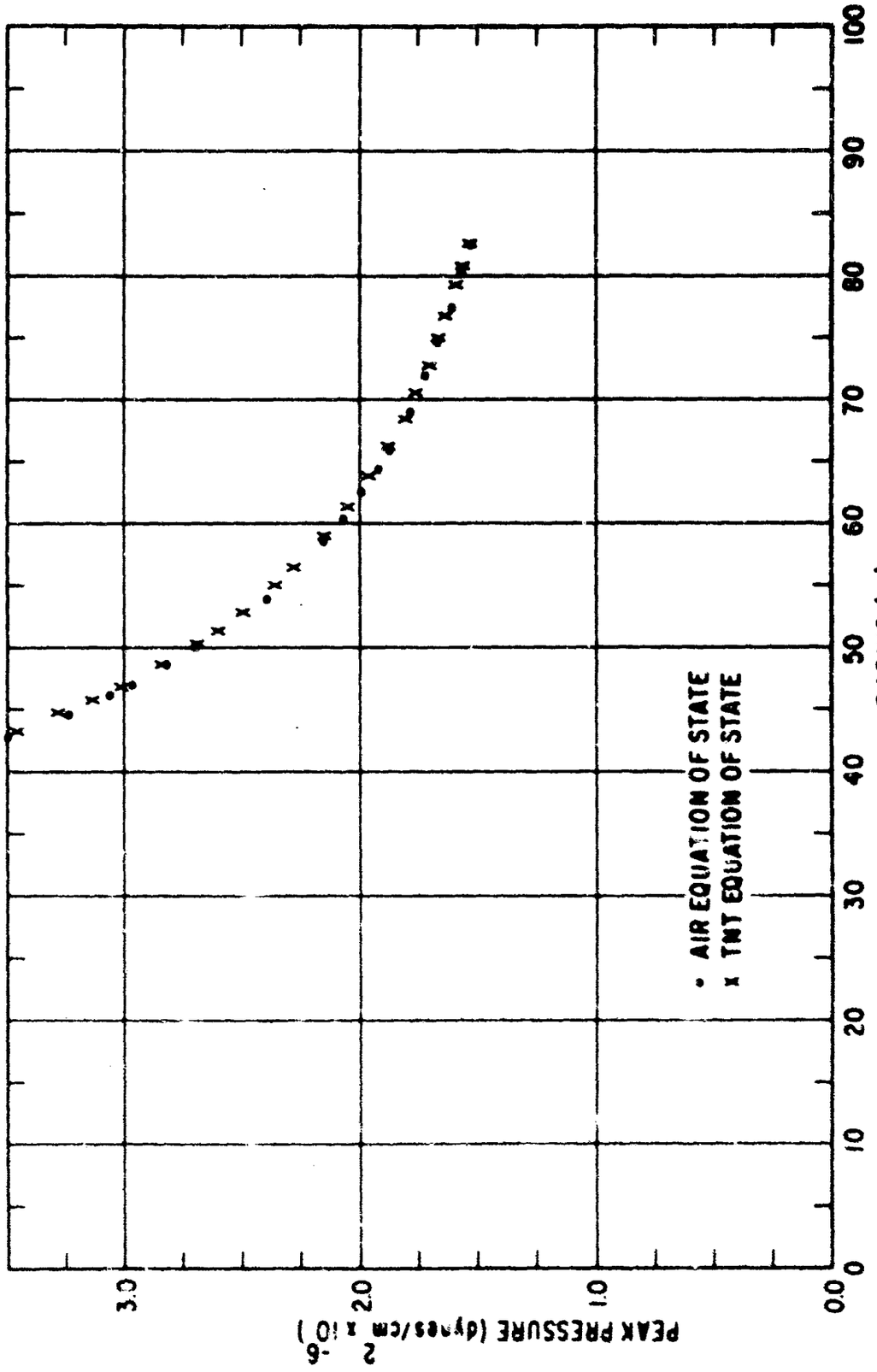

Figure 7. Comparison of Peak Pressure vs. Radius for the Equations of State for TNT and Air.

3. Comparison of the Methane and TNT Results

Both runs were made on identical grids, the only difference being the input conditions from the SAP calculation. In both cases an interface of trace particles was placed at the gas-air interface.

This interface brings to light the first notable difference in the calculation. The high density TNT expanding into the low density air gives rise to Taylor instabilities at the interface. These can be clearly seen on the TNT plots. Since the methane-oxygen mixture has nearly the same density as air, the above condition does not exist, and in fact is not seen in the calculation.

The overpressure for TNT at a radius of 16.8 meters is less than that for methane at the same radius. At a radius of 26 meters the TNT overpressure exceeds that of the methane. This is due to the somewhat larger kinetic energy of the TNT shock.

Although the peak pressure and peak dynamic pressure of the TNT shock are greater than that of methane to a radius of 34 meters, the impulses in both cases are larger for the methane than for TNT. This means that the shock from methane is much thicker than that of TNT.

SECTION VI

CONCLUSIONS

The SAP and SHELL codes have, in past calculations, reproduced the phenomenology of atmospheric blast both quantitatively and qualitatively. Results have agreed with experimental data to within 10 percent. Therefore, there is considerable confidence in the results reported here.

As can be seen in figures 8 and 9 there is agreement between SAP and SHELL overpressures, and both are from 3 percent to 20 percent higher than Brode's (Ref 16). The dynamic pressures, velocities and impulses are good to within 5 percent. The calculated arrival time for station 1 agrees with Brode's arrival time to within 2 percent.

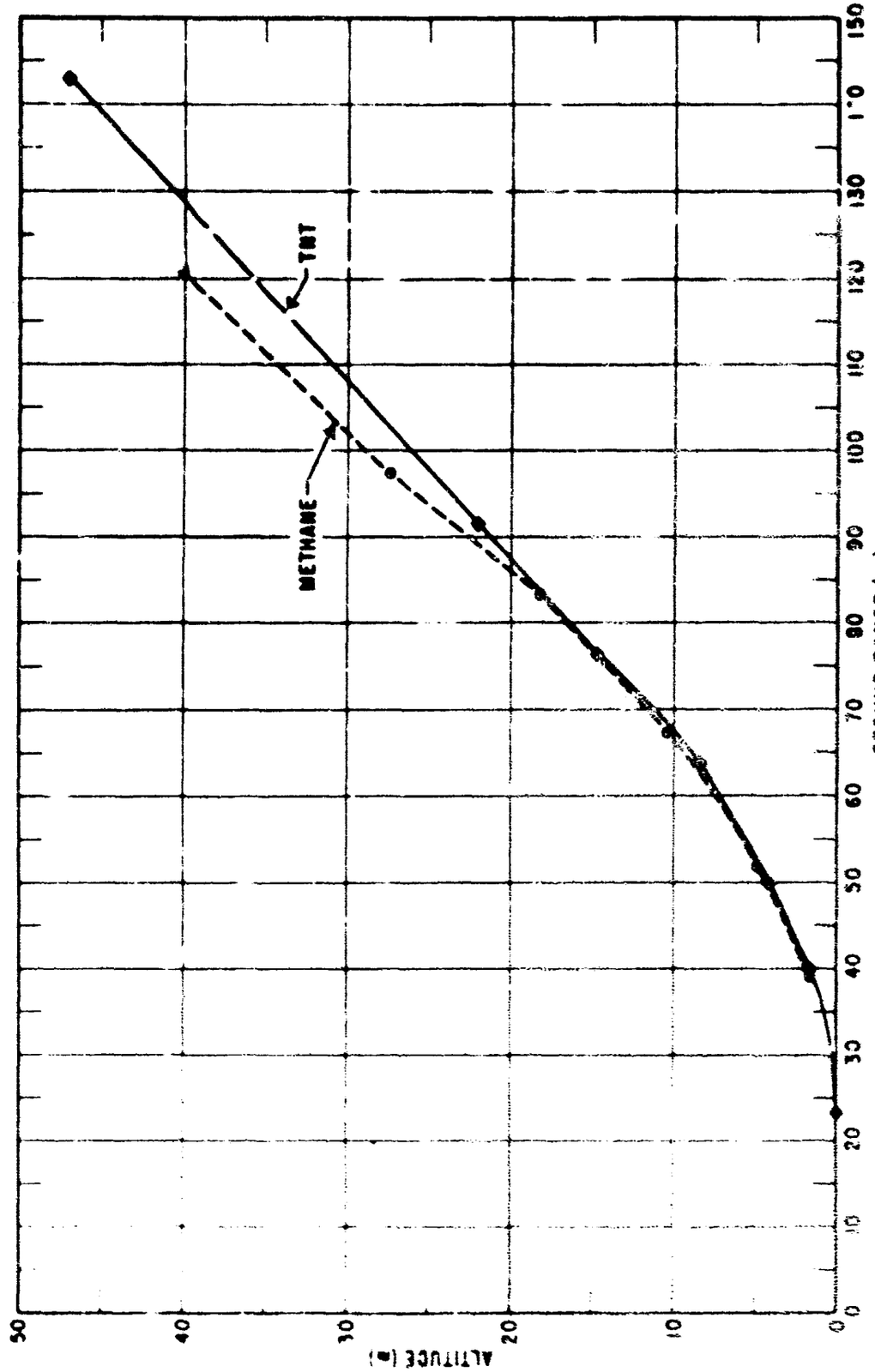

Figure 8. Triple-Point Path.

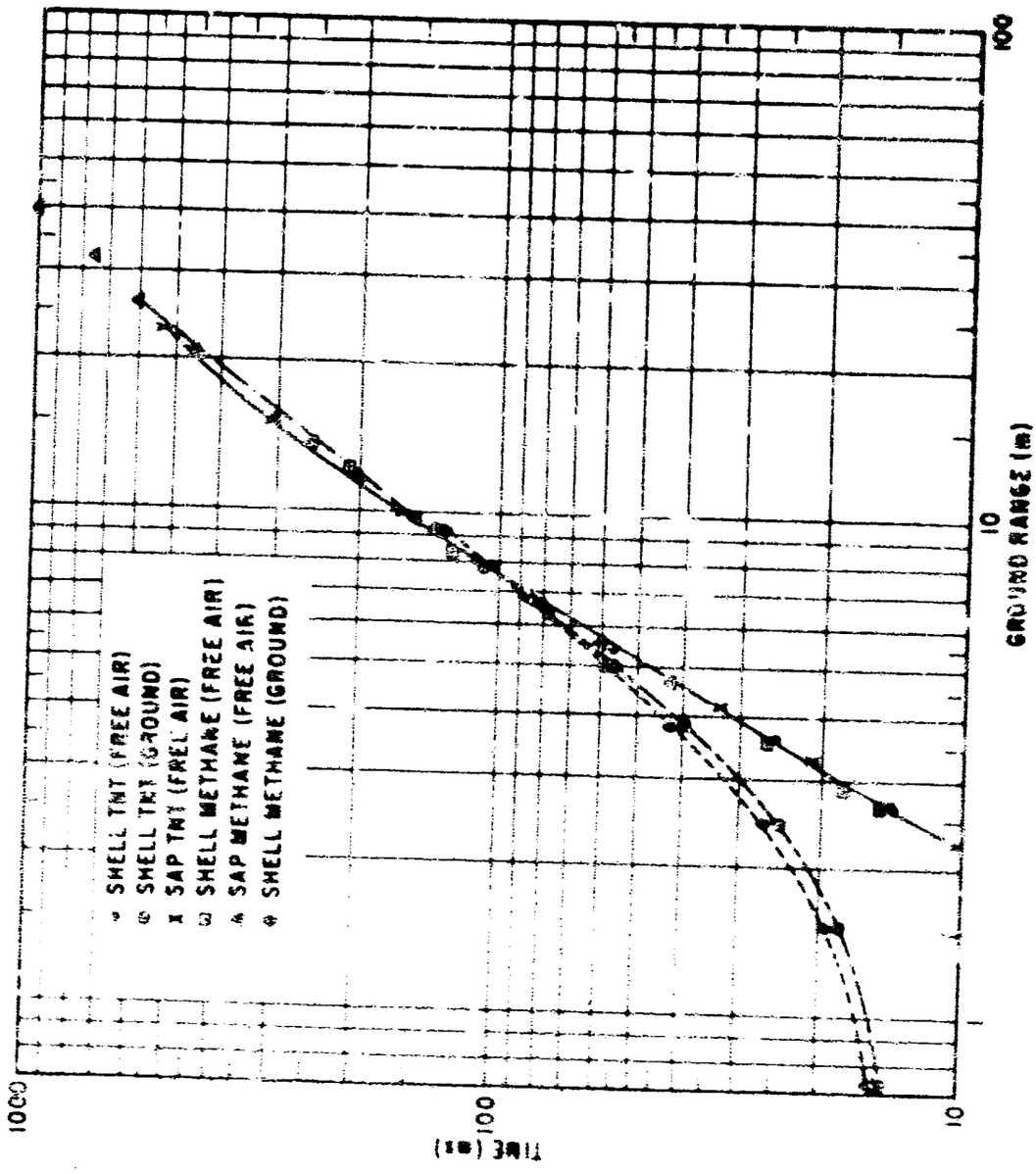

Figure 9. Arrival Time vs. Ground Range.

This page intentionally left blank.

APPENDIX

This appendix presents a summary of the calculation in graphical form. This information was obtained from the detailed history of the calculation contained in Volume II.

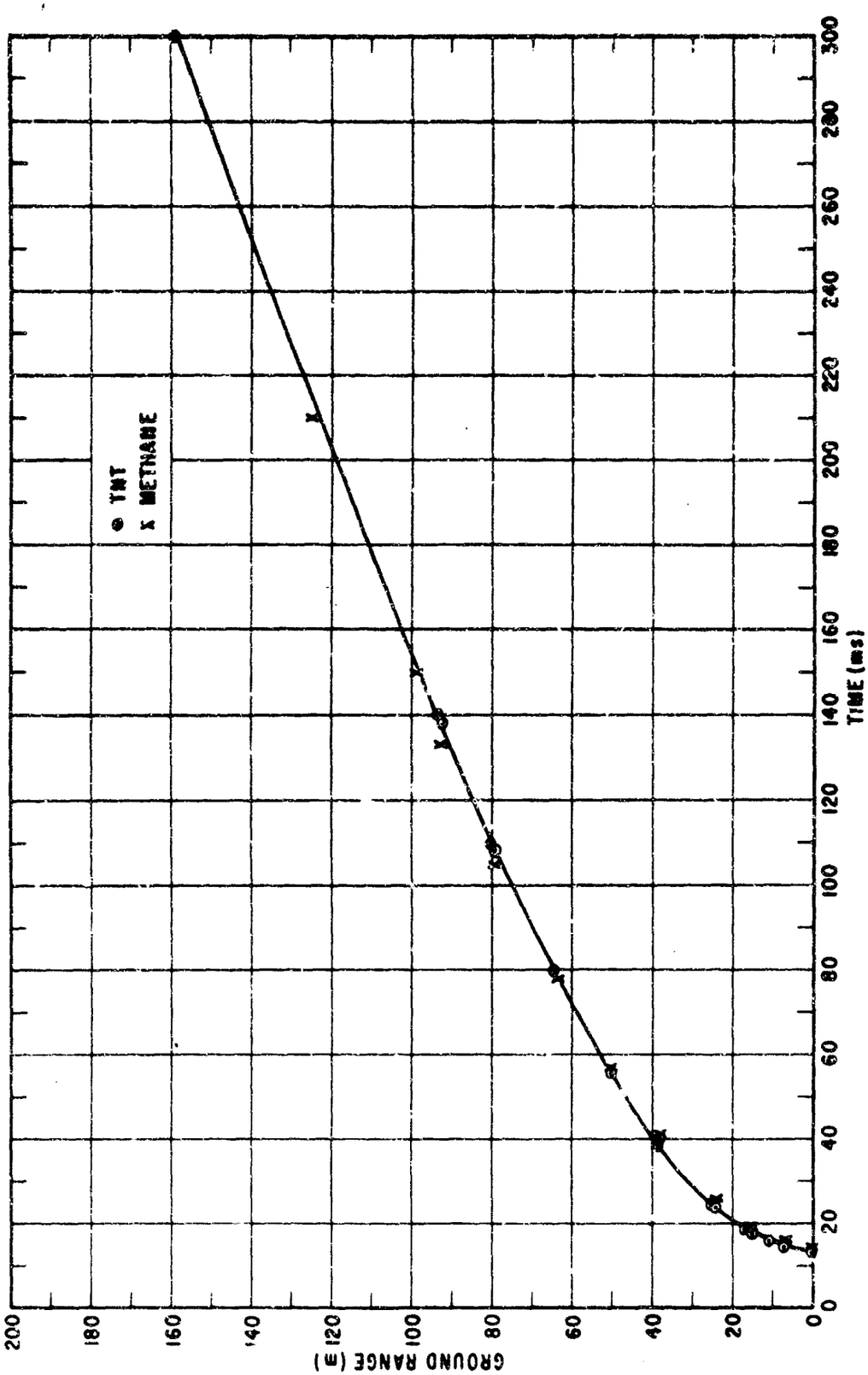

Figure 10. Ground Range vs. Time.

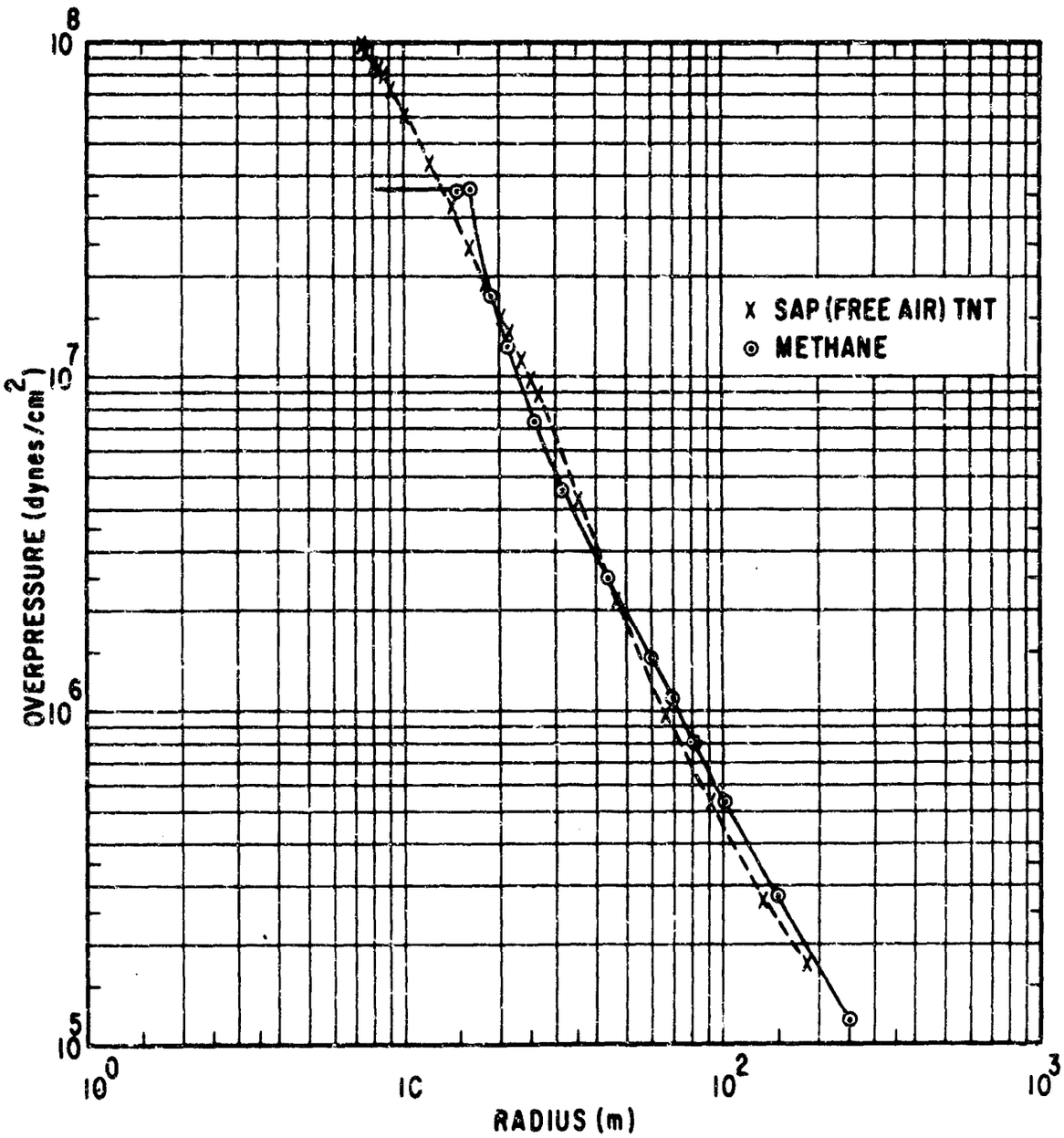

Figure 11. Methane-TNT Overpressures vs. Radius.

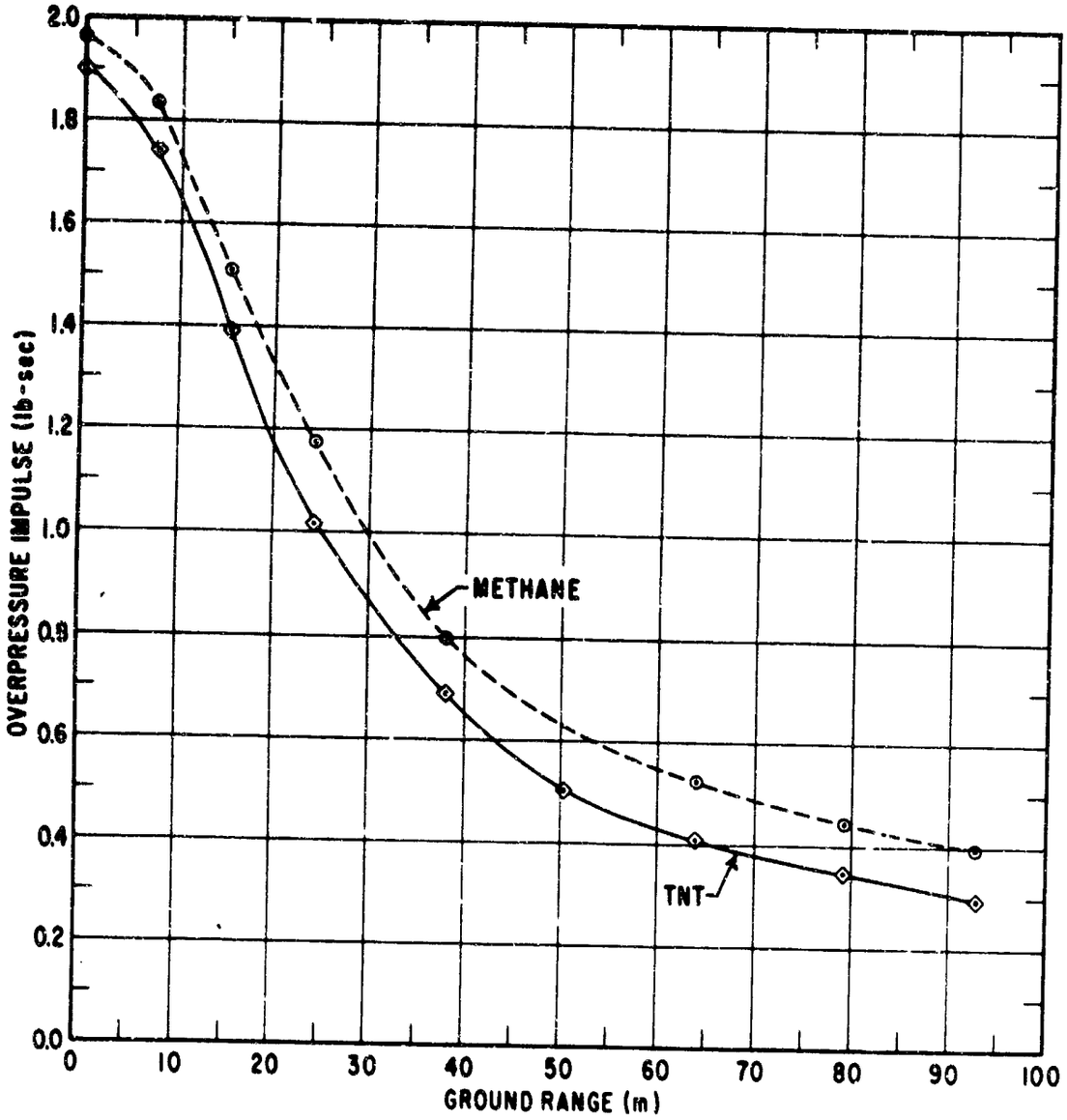

Figure 12. Ground Level Overpressure Impulse vs. Ground Range.

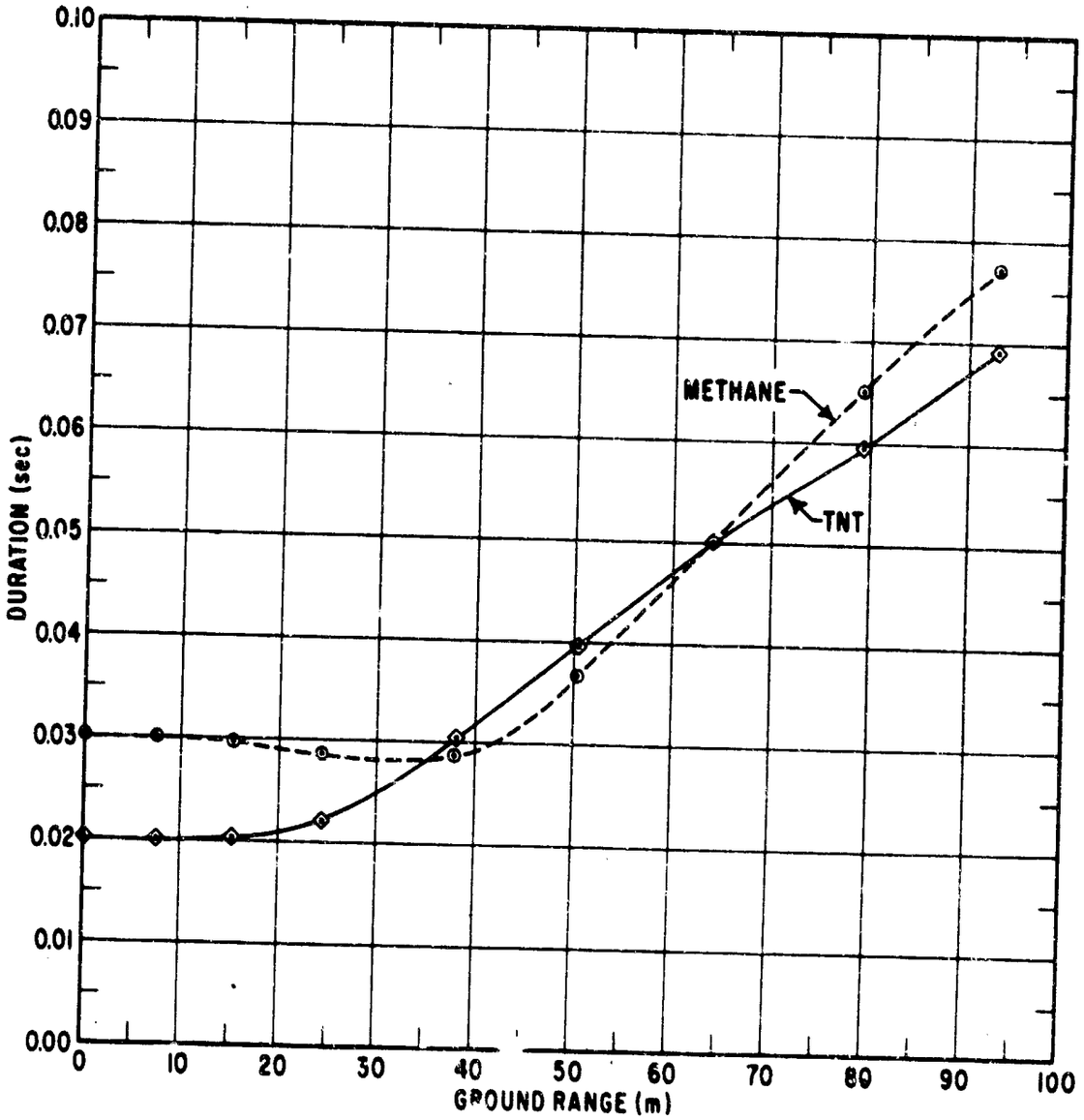

Figure 13. Positive Phase Duration vs. Ground Range.

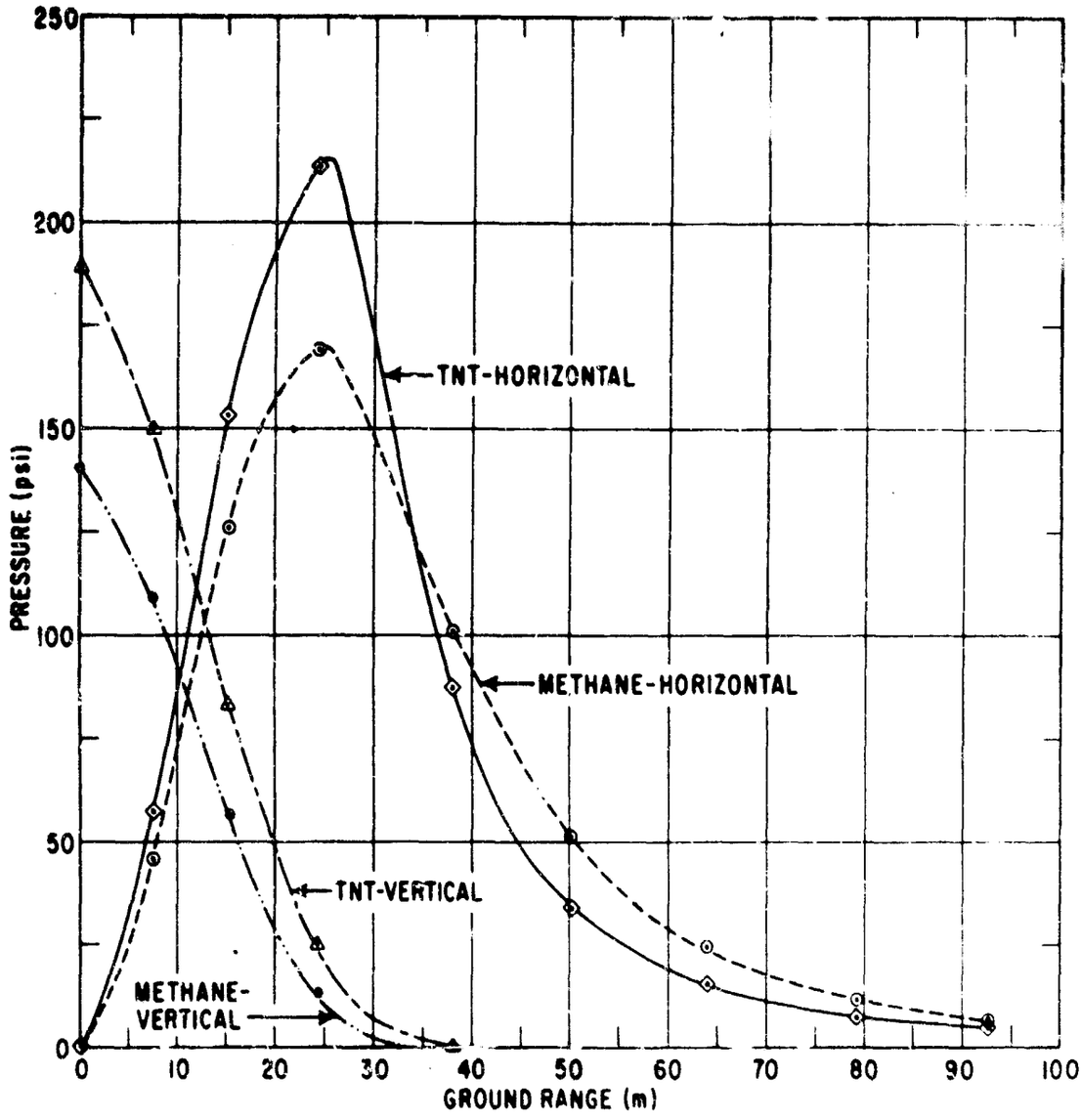

Figure 14. Dynamic Pressure vs. Ground Range.

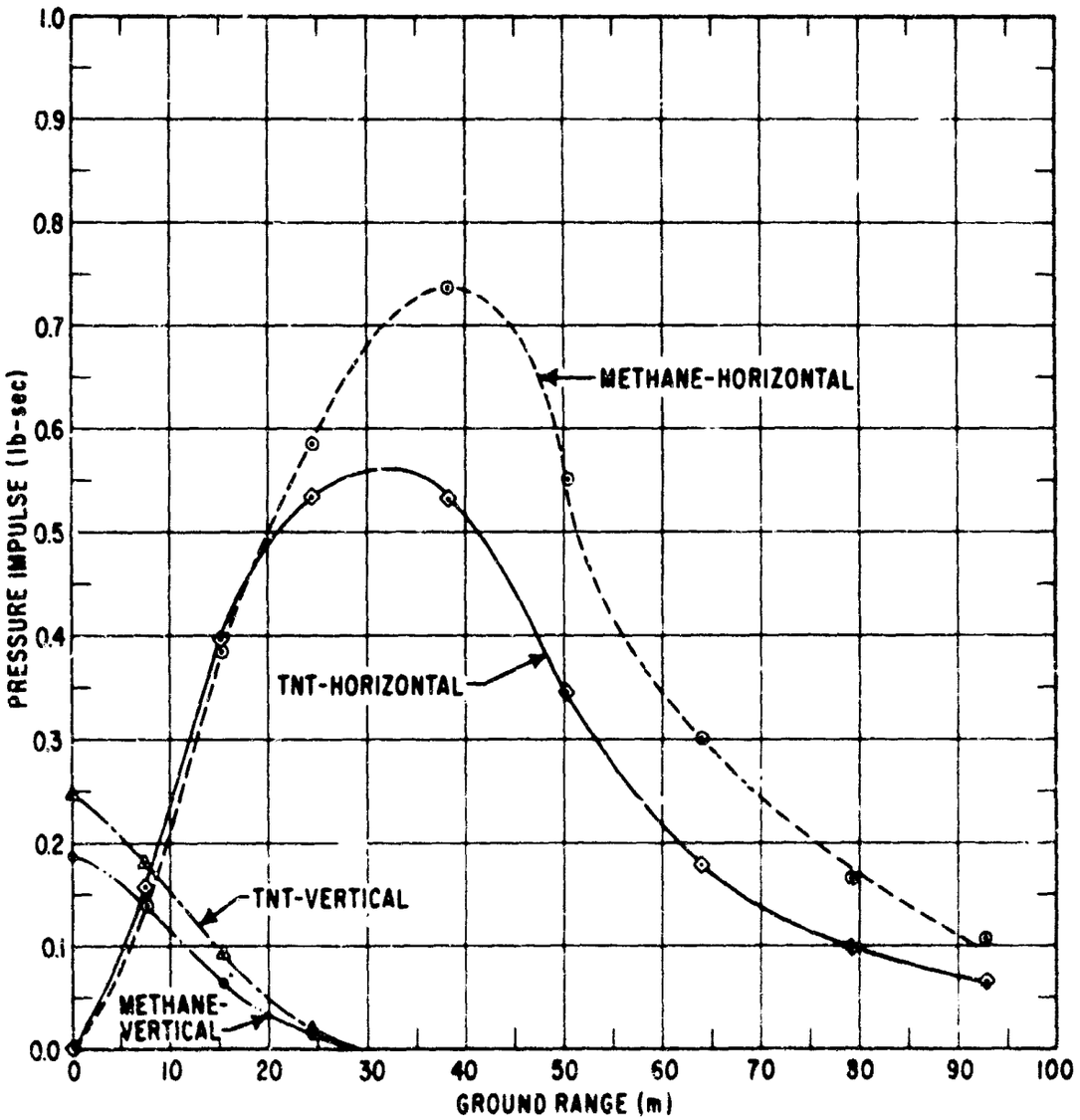

Figure 15. Dynamic Pressure Impulse vs. Ground Range.

REFERENCES

1. Whitaker, W. A., B. S. Chambers III, C. M. Gillespie, et al., (U) Theoretical Calculations of Early Phenomenology--BLUEGILL, AFWL-TDR-64-70, Air Force Weapons Laboratory, Kirtland AFB, New Mexico, July 1964. (S-RD Report)

2. Nawrocki, E. A., W. A. Whitaker, and C. E. Needham. (U) Theoretical Calculations of Late Phenomenology--BLUEGILL, AFWL-TR-65-154, Air Force Weapons Laboratory, Kirtland AFB, New Mexico, October 1965. (S-RD Report)

3. Grandey, R. A., (U) PUFF-VTS Computer Program, AFSWC-TDR-62-76, Air Force Special Weapons Center, Kirtland AFB, New Mexico. February 1963. (Confidential Report)

4. Brodie, R. N. and J. E. Hormuth, PUFF-66 and P-PUFF-66 Computer Programs, AFWL-TR-66-48. Air Force Weapons Laboratory, Kirtland AFB, New Mexico, June 1966.

5. Nance, O., (U) An X-Ray Effects Code, UCRL-5616-T. Ernest O. Lawrence Radia- Laboratory, Livermore, California, July 1959. (S-RD Report)

6. Hisenrath, J., M. S. Green, and C. W. Beckett, Thermodynamic Properties of Highly Ionized Air, SWC-TR-56-35, National Bureau of Standards, Washington, D.C., April 1957.

7. Doan, L. R. and G. H. Nickel, A Subroutine for the Equation of State of Air, RTD(WLR) TM-63-2, Air Force Weapons Laboratory, Kirtland AFB, New Mexico, May 1963.

8. Harlow, F. H., "The Particle-in-Ali Computing Method for Fluid Dynamics," in Fundamental Methods in Hydrodynamics (Methods in Computational Physics, Volume 3, B. Alder S. Fernbach, and M. Rotenberg, editors). p.319, Academic Press, New York, 1964.

9. Johnson, W. E., OIL--A Continuous Two-Dimensional Hydrodynamic Code, GAMD-5580, General Atomic/General Dynamics, San Diego, California, October 1964.

10. Von Neumann, J. and R. D. Richtmeyer, A Method for the Numerical Calculation of Hydrodynamic Shocks, Journal of Applied Physics, Volume 21, p.232, 1950.

11. Bjork, R., N. Brooks and R. Papetti, A Numerical Technique for Solution of Multidimension Hydrodynamic Problems, RM-2628-PR, Rand Corporation, Santa Monica, California, December 1963.

12. Lutzky, M., The Flow Field Behind a Spherical Detonation in TNT Using the Landau-Stanyukovich Equation of State for Detonation Products, NOLTR 64-40, U.S. Naval Ordnance Laboratory, White Oak, Maryland, February 1965.

13. Balcerzak, M. J. and M. R. Johnson, (U) The Investigation of the Detonation-Shock-Tube Technique, WL TDR-64-76, Air Force Weapons Laboratory, Kirtland AFB, New Mexico, February 1965. (S-RD Report)

REFERENCES (cont'd)

14. Zeldovich, I. B. and A. S. Kompaneets, Theory of Detonation, Academic Press, Inc., New York, 1960.

15. U. S. Standard Atmosphere-1962, U.S. Government Printing Office, Washington, D. C., 1962.

16. Brode, H. L., A Calculation of the Blast Wave from a Spherical Change of TNT, RM-1965, Rand Corporation, Santa Monica, California, August 1957.

17. Moulton, J. F. Jr., (U) Nuclear Weapons Blast Phenomena, DASA 1200, Volume 1, U. S. Naval Ordnance Laboratory, Silver Spring, Maryland, March 1960. (S-RD Report)

DISTRIBUTION

Copies

HEADQUARTERS USAF

Hq USAF, Wash, DC 20330

1 (AFOCE)

1 (AFTAC)

1 USAF Dep, The Inspector General (AFIDI), Norton AFB, Calif 92409

1 USAF Directorate of Nuclear Safety (AFINS), Kirtland AFB, NM 87117

MAJOR AIR COMMANDS

AFSC, Andrews AFB, Wash, DC 20331

1 (SCTR)

1 (SCTN)

1 AUL, Maxwell AFB, Ala 36112

USAFA, Colo 80840

1 (FJSRL, OAR)

1 (DFLBA)

AFSC ORGANIZATIONS

1 AFSC Scientific and Technical Liaison Office, Research and Technology Division, AFUPO, Los Angeles, Calif 90045

1 AF Materials Laboratory, Wright-Patterson AFB, Ohio 45433

1 AF Aero-Propulsion Laboratory, Wright-Patterson AFB, Ohio 45433

1 RTD (RTS), Bolling AFB, Wash, DC 20332

AF Msl Dev Cen, Holloman AFB, NM 88330

1 (RRRT)

1 (MDSTT/Mr. Carew)

1 ESD (ESTI), L. G. Hanscom Fld, Bedford, Mass 01731

1 APGC (PGBPS-12), Eglin AFB, Fla 32542

KIRTLAND AFB ORGANIZATIONS

AFSWC, Kirtland AFB, NM 87117

1 (SWEH)

1 (SWT)

DISTRIBUTION (cont'd)

No. cys

AFWL, Kirtland AFB, NM 87117

10 (WLIL)
1 (WLAA)
1 (WLAW)
1 (WLDC)
1 (WLDM)
1 (WLRB/Mr. Murpny)
6 (WLRE/Lt Fisher)
1 (WLRP)
20 (WLRT)
1 (WLX)

OTHER AIR FORCE AGENCIES

Director, USAF Project RAND, via: Air Force Liaison Office, The RAND Corporation, 1700 Main Street, Santa Monica, Calif 90406

1 (RAND Physics Div)
1 (RAND Library)
1 OAR (RROS), 1400 Wilson Blvd, Arlington, Va 22209
1 AFOSR (SRGL), 1400 Wilson Blvd, Arlington, Va 22209
1 AFCRL, L. G. Hanscom Fld, Bedford, Mass 01731

ARMY ACTIVITIES

1 Chief of Research and Development, Department of the Army (CRD/P, Scientific and Technical Information Division), Wash, DC 20310
1 Commanding Officer, Harry Diamond Laboratories, ATTN: Library, Wash, DC 20438

Redstone Scientific Information Center, US Army Missile Command, Redstone Arsenal, Ala 35809

1 (Chief, Document Section)
1 (NIKE-X Project Officer/Mr. H.L. Solomonson, Jr.)

Commanding Officer, Ballistic Research Laboratories, Aberdeen Proving Ground, Md 21005

2 (AMXBR-TB, Mr. J. Meszaros)
2 (Mr. J. R. Kelso)
2 (Mr. R. Reisler)
10 (Mr. J. Keefer)
1 (Air Force Liaison Ofc)

DISTRIBUTION (cont'd)

No. cys	
1	(Marine Corps Liaison Ofc)
1	(Navy Liaison Ofc)
1	(CDC Liaison Ofc)
1	Director, Army Research Office, 3045 Columbia Pike, Arlington, Va 22204
1	Director, US Army Waterways Experiment Sta (WESRL), P.O. Box 631, Vicksburg, Miss 39181
2	Director, US Army Engineer Research and Development Laboratories, ATTN: STINFO Branch, Ft Belvoir, Va 20260
1	Commanding General, White Sands Missile Range (Tech Library), White Sands, NM 88002

NAVY ACTIVITIES

1	Chief of Naval Research, Department of the Navy, Wash, DC 20390
1	Naval Air Systems Command (RRNU), Department of the Navy, Wash, DC 20360
1	Commanding Officer, Naval Research Laboratory, Wash, DC 20390
1	Commanding Officer and Director, David Taylor Model Basin, Wash, DC 20007
1	Superintendent, US Naval Postgraduate School, ATTN: George R. Luckett, Monterey, Calif 93940
1	Commanding Officer and Director, Naval Civil Engineering Laboratory, Port Hueneme, Calif 93041
1	Commanding Officer and Director, Naval Applied Science Laboratory, Brooklyn, NY 11251
1	Commander, Naval Ordnance Test Station (Code 753), China Lake, Calif 93557
1	Commander, Naval Ordnance Laboratory, ATTN: Dr. Rudlin, White Oak, Silver Spring, Md 20910
1	Officer-in-Charge, Naval Civil Engineering Corps Officers School, US Naval Construction Battalion Center, Port Hueneme, Calif 93041
1	Commanding Officer, US Naval Explosive Ordnance Disposal Facility, US Naval Propellant Plant, Indian Head, Md 20640
1	Office of Naval Research, Wash, DC 20360
1	Director of Naval Warfare Analyses, Institute of Naval Studies, Office of the Chief of Navy Ops, 545 Technology Square, Cambridge, Mass 02139
1	Commanding Officer, NWEF (Code WE), Kirtland AFB, NM 87117

OTHER DOD ACTIVITIES

	Director, DASA, Wash, DC 20301
2	(Document Library Branch)

DISTRIBUTION (cont'd)

No. cys	
1	(Mr. Mort Rubenstein)
1	(Capt Choromokos)
1	(Col Brown)
1	(Dr Wikner)
1	Commander Field Command, DASA (FCAG3, Special Weapons Publication Distribution), Sandia Base, NM 87115
1	Office of Director of Defense Research and Engineering, ATTN: John E. Jackson, Office of Atomic Program, Rm 3E1071, The Pentagon, Wash, DC 20330
20	DDC (TIAAS), Cameron Station, Alexandria, Va 22314

AEC ACTIVITIES

1	US Atomic Energy Commission (Hq Library, Reports Section), Mail Station G-017, Wash, DC 20545
	Sandia Corporation, Box 5800, Sandia Base, NM 87115
2	(Information Distribution Division/Mr. M.L. Merritt)
1	(Mr. D.R. Breding/Div 7242)
2	Sandia Corporation (Tech Library), P.O. Box 969, Livermore, Calif 94551
2	University of California Lawrence Radiation Laboratory (Tech Info Div, Attn: Dr. R.K. Wakerling), Berkeley, Calif 94720
2	Director, Los Alamos Scientific Laboratory (Helen Redman, Report Library), P.O. Box 1663, Los Alamos, NM 87554

OTHER

1	Langley Research Center (NASA), ATTN: Associate Director, Langley Station, Hampton, Va 23365
1	Manned Spacecraft Center (NASA), ATTN: Chief, Tech Info Div, Houston, Tex 77001
1	Institute for Defense Analysis, Rm 2B257, The Pentagon, Wash, DC 20330 THRU: ARPA
	Massachusetts Institute of Technology, Lincoln Laboratory, P.O. Box 73, Lexington, Mass 02173
1	(Document Library)
1	(MIT Aeroelastic Structures Lab/Mr. Frank Durgan)
1	Aerospace Corporation, P.O. Box 95085, Los Angeles, Calif 90045
1	Aerospace Corporation, ATTN: Ali M. Naqvi, San Bernardino Operations, P.O. Box 1308, San Bernardino, Calif 92402
1	Eric H. Wang Civil Engineering Research Facility, ATTN: Dr. Zwoyer, Box 188, University Station, Albuquerque, NM 87103
1	Applied Physics Laboratory, The Johns Hopkins University, 8621 Georgia Avenue, Silver Spring, Md 20910

DISTRIBUTION (cont'd)

No. cys	
1	Forrestal Research Center Library, Aeronautical Sciences Bldg, Princeton University, Princeton, NJ 08540
1	General Atomic Division, General Dynamics Corporation, 10955 John Jay Hopkins Drive, San Diego, Calif 92121
1	General Electric TEMPO, ATTN: Mr. Bill Hart, 735 State Street, Santa Barbara, Calif 93101
1	College Park Metallurgy Center, US Bureau of Mines, ATTN: Library, College Park, Md 20740
1	University of Massachusetts, Head, Civil Engineering Dept, Amherst, Mass 01002
1	University of Michigan, University Research Security Office, Lobby 1, East Engineering Bldg, Ann Arbor, Mich 48106
1	Space Technology Laboratories, Inc., STLTD, ATTN: Mr. F. A. Pieper, Bldg S/1930, One Space Park, Redondo Beach, Calif 90278
	Stanford Research Institute, Menlo Park, Calif 94025
1	(Mr. T. D. Witherly)
1	(Mr. E. Wood)
	TRW Systems, One Space Park, Redondo Beach, Calif 90278
1	(ATTN: Burt Peterson)
1	(ATTN: Library)
	Bell Telephone Laboratories, Whippany, NJ 07981
10	(Mr. William W. Troutman)
1	(Mr. T. Gressitt)
1	General American Transportation Co., General American Research Div, ATTN: Mr. Milton R. Johnson, GATX 7501 N. Natchez Ave, Niles Ill 60648
1	Physics International Co., ATTN: Mr. D. Andrews, 2700 Merced St., San Leandro, Calif 94577
1	Bechtel Corporation, 4550 Seville Ave, ATTN: Mr. William G. Bingham,Jr., Vernon,Calif 90058
1	The Boeing Company, ATTN: Mr. R. H. Carlson, Seattle, Wash 98124
1	General American Transportation Corp., ATTN: Lib, MRD Div, 7501 North Natchez Ave, Niles, Ill 60648
1	Holmes & Narver, Inc., Special Projects Division, ATTN: Mr. S. B. Smith, 849 South Broadway, Los Angeles, Calif 90014
2	United Research Services, 1811 Trousdale Drive, Burlingame, Calif 94010
1	Southwest Research Institute, ATTN: Mr. M.L. Whitfield, 8500 Culebra Road, San Antonio, Tex 78228

DISTRIBUTION (cont'd)

No. cys	
1	The University of Michigan, ATTN: Univ Rsch Scty Ofc, Ann Arbor, Mich 48104
1	University of Michigan Institute of Science & Technology, ATTN: Mr. Gordon Krantti, P.O. Box 618, Ann Arbor, Michigan 48104
1	Princeton University, Palmer Physical Laboratory, ATTN: Dr. Walker Bleakney, Princeton, NJ 08540
1	Massachusetts Institute of Technology, ATTN: Dr. Robert Hansen, 77 Massachusetts Ave, Cambridge, Mass 02139
1	St Louis University, ATTN: Dr. Carl Kisslinger, 221 North Grand, St Louis, Missouri 63100
1	University of Illinois,Talbot Laboratory, ATTN: Dr. N.M. Newmark, Rm 207, Urbana, Ill 61803
1	IIT Research Institute, ATTN: Dr. Eugene Sevin, 10 W. 35th Street, Chicago, Ill 60616
1	Official Record Copy (WLRTH/Capt Whitaker)

This page intentionally left blank.

Unclassified

Security Classification

DOCUMENT CONTROL DATA - R&D

(Security classification of title, body of abstract and indexing annotation must be entered when the overall report is classified)

1. ORIGINATING ACTIVITY (Corporate author) Air Force Weapons Laboratory (WLRTH) Kirtland Air Force Base, New Mexico	2a. REPORT SECURITY CLASSIFICATION Unclassified 2b. GROUP

3. REPORT TITLE

THEORETICAL CALCULATIONS OF THE PHENOMENOLOGY OF HE DETONATIONS

4. DESCRIPTIVE NOTES (Type of report and inclusive dates)

1 September 1965 to 1 June 1966

5. AUTHOR(S) (Last name, first name, initial)

Whitaker, William A., Capt, USAF; Nawrocki, Edmund A., Capt, USAF; Needham, Charles E.; Troutman, William W.

6. REPORT DATE	7a. TOTAL NO. OF PAGES	7b. NO. OF REFS
November 1966	62	17

8a. CONTRACT OR GRANT NO.	9a. ORIGINATOR'S REPORT NUMBER(S)
b. PROJECT NO. 5710	AFWL-TR-66-141, Vol. I
c. Subtask 1.027	9b. OTHER REPORT NO(S) (Any other numbers that may be assigned this report)
d.	

10. AVAILABILITY/LIMITATION NOTICES This document is subject to special export controls and each transmittal to foreign governments or foreign nationals may be made only with prior approval of AFWL (WLRTH), Kirtland AFB, N.M. Distribution of this document is limited because of the technology discussed.

11. SUPPLEMENTARY NOTES	12. SPONSORING MILITARY ACTIVITY
	AFWL (WLRTH) Kirtland AFB NM 87117

13. ABSTRACT

The phenomenology of two atmospheric high-explosive detonations were calculated theoretically. The first was a 20-short-ton spherical charge of TNT (loading density--1.56 gms/cc). The second was a methane-oxygen mixture (mole ratio 1 to 1.5) contained in a 55-ft-radius balloon. Both detonations took place at an altitude of 670 meters (ambient pressure 13.6 psi) with a reflecting surface 85 feet below burst point. The calculations, taken out to 300 milliseconds after detonations, were performed by using SAP, a one-dimensional Lagrangian hydrodynamic code and SHELL-OIL, a two-dimensional pure Eulerian hydrodynamic code. Volume II of this report contains the details of the results in graphical form. Included are pressure and density contours, velocity vector plots, and wave forms for 19 test stations.

DD FORM 1 JAN 64 1473

Unclassified

Security Classification

Unclassified

Security Classification

14. KEY WORDS	LINK A ROLE	LINK A WT	LINK B ROLE	LINK B WT	LINK C ROLE	LINK C WT
Blast Wave						
Shock Reflection						
Mach Reflection						
Triple Point						
HE Detonation, Calculation of						
SAP						
SHELL-OIL						

INSTRUCTIONS

1. ORIGINATING ACTIVITY: Enter the name and address of the contractor, subcontractor, grantee, Department of Defense activity or other organization *(corporate author)* issuing the report.

2a. REPORT SECURITY CLASSIFICATION: Enter the overall security classification of the report. Indicate whether "Restricted Data" is included. Marking is to be in accordance with appropriate security regulations.

2b. GROUP: Automatic downgrading is specified in DoD Directive 5200.10 and Armed Forces Industrial Manual. Enter the group number. Also, when applicable, show that optional markings have been used for Group 3 and Group 4 as authorized.

3. REPORT TITLE: Enter the complete report title in all capital letters. Titles in all cases should be unclassified. If a meaningful title cannot be selected without classification, show title classification in all capitals in parenthesis immediately following the title.

4. DESCRIPTIVE NOTES: If appropriate, enter the type of report, e.g., interim, progress, summary, annual, or final. Give the inclusive dates when a specific reporting period is covered.

5. AUTHOR(S): Enter the name(s) of author(s) as shown on or in the report. Enter last name, first name, middle initial. If military, show rank and branch of service. The name of the principal author is an absolute minimum requirement.

6. REPORT DATE: Enter the date of the report as day, month, year; or month, year. If more than one date appears on the report, use date of publication.

7a. TOTAL NUMBER OF PAGES: The total page count should follow normal pagination procedures, i.e., enter the number of pages containing information.

7b. NUMBER OF REFERENCES: Enter the total number of references cited in the report.

8a. CONTRACT OR GRANT NUMBER: If appropriate, enter the applicable number of the contract or grant under which the report was written.

8b, 8c, & 8d. PROJECT NUMBER: Enter the appropriate military department identification, such as project number, subproject number, system numbers, task number, etc.

9a. ORIGINATOR'S REPORT NUMBER(S): Enter the official report number by which the document will be identified and controlled by the originating activity. This number must be unique to this report.

9b. OTHER REPORT NUMBER(S): If the report has been assigned any other report numbers *(either by the originator or by the sponsor)*, also enter this number(s).

10. AVAILABILITY/LIMITATION NOTICES: Enter any limitations on further dissemination of the report, other than those imposed by security classification, using standard statements such as:

(1) "Qualified requesters may obtain copies of this report from DDC."

(2) "Foreign announcement and dissemination of this report by DDC is not authorized."

(3) "U. S. Government agencies may obtain copies of this report directly from DDC. Other qualified DDC users shall request through ______________."

(4) "U. S. military agencies may obtain copies of this report directly from DDC. Other qualified users shall request through ______________."

(5) "All distribution of this report is controlled. Qualified DDC users shall request through ______________."

If the report has been furnished to the Office of Technical Services, Department of Commerce, for sale to the public, indicate this fact and enter the price, if known.

11. SUPPLEMENTARY NOTES: Use for additional explanatory notes.

12. SPONSORING MILITARY ACTIVITY: Enter the name of the departmental project office or laboratory sponsoring *(paying for)* the research and development. Include address.

13. ABSTRACT: Enter an abstract giving a brief and factual summary of the document indicative of the report, even though it may also appear elsewhere in the body of the technical report. If additional space is required, a continuation sheet shall be attached.

It is highly desirable that the abstract of classified reports be unclassified. Each paragraph of the abstract shall end with an indication of the military security classification of the information in the paragraph, represented as *(TS)*, *(S)*, *(C)*, or *(U)*.

There is no limitation on the length of the abstract. However, the suggested length is from 150 to 225 words.

14. KEY WORDS: Key words are technically meaningful terms or short phrases that characterize a report and may be used as index entries for cataloging the report. Key words must be selected so that no security classification is required. Identifiers, such as equipment model designation, trade name, military project code name, geographic location, may be used as key words but will be followed by an indication of technical context. The assignment of links, rules, and weights is optional.